AD_____

Award Number: DAMD17-03-1-0473

TITLE: Stromal Gene Expression and Function in Primary Breast Tumors that Metastasize to Bone Cancer

PRINCIPAL INVESTIGATOR: Belinda S Parker, Ph.D.

CONTRACTING ORGANIZATION: University of Melbourne
Victoria, Australia 3010

REPORT DATE: July 2006

TYPE OF REPORT: Annual Summary

PREPARED FOR: U.S. Army Medical Research and Materiel Command
Fort Detrick, Maryland 21702-5012

REPORT DOCUMENTATION PAGE

Form Approved
OMB No. 0704-0188

1. REPORT DATE	2. REPORT TYPE	3. DATES COVERED
01-07-2006	Annual Summary	1 Jul 2003 – 30 Jun 2006

4. TITLE AND SUBTITLE

Stromal Gene Expression and Function in Primary Breast Tumors that Metastasize to Bone Cancer

5a. CONTRACT NUMBER

5b. GRANT NUMBER
DAMD17-03-1-0473

5c. PROGRAM ELEMENT NUMBER

6. AUTHOR(S)

Belinda S Parker, Ph.D.

5d. PROJECT NUMBER

5e. TASK NUMBER

5f. WORK UNIT NUMBER

7. PERFORMING ORGANIZATION NAME(S) AND ADDRESS(ES)

University of Melbourne
Victoria, Australia 3010

8. PERFORMING ORGANIZATION REPORT NUMBER

9. SPONSORING / MONITORING AGENCY NAME(S) AND ADDRESS(ES)
U.S. Army Medical Research and Materiel Command
Fort Detrick, Maryland 21702-5012

10. SPONSOR/MONITOR'S ACRONYM(S)

11. SPONSOR/MONITOR'S REPORT NUMBER(S)

12. DISTRIBUTION / AVAILABILITY STATEMENT
Approved for Public Release; Distribution Unlimited

13. SUPPLEMENTARY NOTES
Original contains colored plates: ALL DTIC reproductions will be in black and white.

14. ABSTRACT Tumor progression and metastasis is mediated not only by tumor cells but by the surrounding stroma as well, including the vascular endothelium. Knowledge of the molecular and cellular interactions that promote metastasis is required to determine prognostic markers and therapeutic targets for metastatic breast cancer. A clinically relevant syngeneic model of breast cancer metastasis has been used to determine gene expression alterations that occur in both tumor epithelial cells and the associated vascular endothelium throughout metastatic progression. A number of candidates have been identified as over-expressed or suppressed in tumor endothelium and in the tumor cells themselves during metastatic progression. Some of these have been verified and are being analysed further for their functional role in metastasis, and for their role in human breast cancer. Of particular interest are 3 groups of genes- the increased expression and activity of cathepsin proteases and their inhibitor Stefin A, suppression of interleukin receptors IL13rα1 and IL4rα and the interferon regulatory factor IRF7 (genes involved in immune defence) and also suppression of a novel gene that may have promise as a metastasis suppressor, Lrch2. In the human disease, our studies have shown that a lack of Stefin A primary tumor expression decreased risk of recurrence and improved patient outcome in a small cohort study.

15. SUBJECT TERMS
breast cancer, metastasis, expression profiling, bone disease

16. SECURITY CLASSIFICATION OF:				18. NUMBER OF PAGES	19a. NAME OF RESPONSIBLE PERSON
					USAMRMC
a. REPORT	b. ABSTRACT	c. THIS PAGE			19b. TELEPHONE NUMBER *(include area code)*
U	U	U	UU	47	

Table of Contents

INTRODUCTION

Breast cancer, although relatively treatable at an early stage, is a clinical problem once it has progressed to metastatic disease in tissues such as lung and bone. It is therefore crucial to determine the molecular mechanism by which primary tumor cells migrate and develop metastases at secondary organs. It is becoming increasingly evident that tumor progression and metastasis is mediated not only by tumor cells but by the surrounding stroma as well (1-4), including the vascular endothelium. Knowledge of the molecular and cellular interactions that promote metastasis is required to determine prognostic markers and therapeutic targets for metastatic breast cancer.

The importance of tumor-stromal interactions to tumorigenesis and metastatic progression has illustrated the absolute requirement for use of *in vivo* models that allow for such an interaction. For this reason conventional cell culture studies *in vitro* have become inadequate, with researchers developing models for 3D cultures (5, 6) that aim to mimic the cellular microenvironment *in vivo*. The ideal model, however, is an *in vivo* model that encompasses the entire process of breast cancer metastasis, including primary tumor formation and spontaneous metastasis to distant sites applicable to the human disease. Additionally, unlike the commonly used human xenograft and intra-cardiac models, the ideal animal model should be syngeneic to ensure tumor and host stroma compatibility and to allow the use of immunocompetent animals. Recent studies have demonstrated that matched host stroma is important in breast development and carcinogenesis (3, 7, 8) and the numerous roles of the immune system in tumorigenesis are well documented (9, 10). The contribution of stroma also raises another important issue. Whole tumor gene expression analysis ignores the contribution of tumor-associated stromal cells to growth and invasion of tumor cells. The use of cell specific profiling is important to identify gene candidates in stromal cells that could have been masked using whole tumor analysis.

Our laboratory has previously developed a spontaneous metastasis model that mimics the clinical disease with primary tumor formation, invasion of cells through the stroma and into the circulation and colonization at distant organs (11, 12). To our knowledge, this is the only syngeneic model of the entire process and has great potential both for gene discovery and as a tool for analysing the functional significance of gene candidates in breast cancer metastasis. Using this model (Figure 1) and immunopurification of specific cell populations and microarray profiling, we have identified gene expression alterations that occur in highly metastatic primary tumor epithelial cells and associated host vascular endothelium (compared to non-metastatic tumors) and also changes that occur in tumor and host cells associated with metastases in bone. We have identified a number of genes aberrantly expressed in these cell populations, including those previously implicated in tumorigenesis and/or metastasis and also novel candidates. We have initiated investigations into the expression and function of a number of genes identified including the cathepsins and their inhibitor Stefin A, 2 novel ESTs and the interferon regulatory factor IRF7. The clinical relevance of this study to the human disease has been verified by further analysis of the cathepsin inhibitor Stefin A. This gene was found in the model upregulated in tumor cells derived from highly metastatic primary tumors and was expressed at even higher levels in matched metastases in lung and bone. Expression of Stefin A in metastatic tumor cells is only induced *in vivo* and is not seen in cells in culture unless co-cultured with appropriate stromal cell populations (ie. mammary fat pad) indicating a role for the microenvironment in its induction. Our studies in human tissues have supported the murine studies, and preliminary data indicates that Stefin A is a marker of metastasis and poor outcome in breast cancer.

The main objectives are to study the molecular events involved in metastasis, specifically we aim to 1) verify gene candidates expressed in both tumor epithelial and tumor-derived endothelial cells that were identified as associated with metastasis, 2) determine whether these candidates are also expressed in human breast cancer, 3) study the function of these genes *in vitro*, 4) explore the role of candidates in distant metastasis to lung and bone *in vivo.*

BODY

<u>TASK 1:</u> Isolate tumor and stromal cells from primary tumors of differing metastatic capacity* and *subject the RNA isolated from these cells to microarray analysis (months 1-12)

a. Purify specific cell populations (epithelial, endothelial and fibroblast cells) using immunopurification from fresh tumors and by laser capture microdissection (LCM) from frozen tumors (months 1-9).
b. Perform microarray analysis of specific cell types, comparing RNA from cells derived from a non-metastatic tumor to that from a metastatic tumor (months 6-12).

We used a clinically relevant syngeneic model of breast cancer metastasis to determine gene expression alterations that occur both between primary breast cancers with varying metastatic potential and between matched primary and bone metastases. For this study, we immunopurified epithelial and endothelial cell populations and profiled them separately to identify a number of tumor and stroma associated genes, some of which have not been associated previously with breast cancer metastasis. During the course of this fellowship a number of microarrays have been performed to identify gene expression alterations associated with metastatic progression. These include comparing tumor cells isolated from highly metastatic primary tumors to those from primary tumors that were non-metastatic. To identify changes in the surrounding microenvironment, endothelial cells were purified from the same tumors to identify changes in the vasculature that may be associated with successful tumor cell dissemination and metastasis. To identify changes that may be required for growth in distant secondary tissues, we have also compared expression of purified tumor cells from matched primary tumors and bone metastases. Again, changes in the surrounding bone microenvironment were investigated by purifying endothelial cells from tumor-burdened and non-tumor burdened spines.

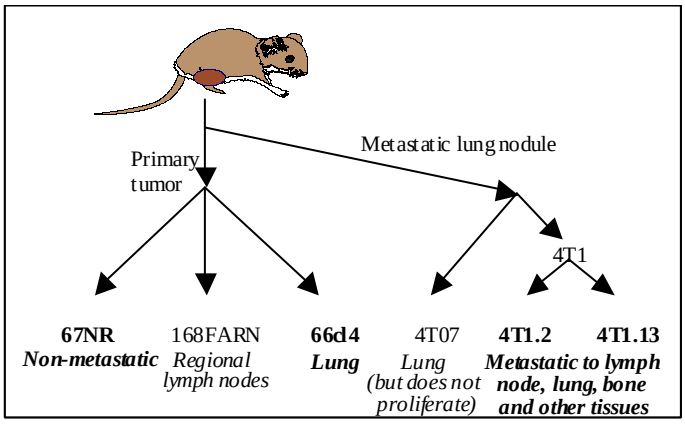

Figure 1. Orthotopic model of breast cancer metastasis to bone. Several tumor sublines have been isolated from a spontaneously arising mammary gland carcinoma. Each subline has a distinct metastatic phenotype. 67NR is non-metastatic, while 168FARN, 66cl4 and 4T07 are weakly metastatic. 4T1.2 and 4T1.13 are two bone metastasizing tumor clones derived from the lung metastasizing 4T1 subline.

1) Primary tumor expression profiling

We have separated epithelial cells, endothelial cells and remaining stromal cells from the primary tumors of the tumor lines shown in Figure 1. The separation was done individually for six tumors of each line following 28 days growth in the mammary gland of Balb/c mice. Fresh resected tissue (normal fat pad, primary tumor tissue or the metastatic sites spine, femur and lung) was obtained and cell separation completed using an immunobead protocol. Epithelial and endothelial cells were isolated as described previously (13) but with the use of mouse pan B and T Dynabeads™ (Dynal Biotech, Norway) for removal of mouse B and T cells and CELLection Epithelial Enrich (Dynal Biotech) for positive selection of epithelial cells. Purity of the epithelial and endothelial cell populations was confirmed by realtime RT-PCR of epithelial (CK18) and endothelial (vWF, P1H12) associated genes (Figure 2). During the cell isolation procedure, epithelial cells, endothelial cells, B and T cells and red blood cells are removed. The composition of the "remaining stromal cells" is likely to be primarily

fibroblasts, with a small number of other cells including macrophages and adipocytes likely to be present.

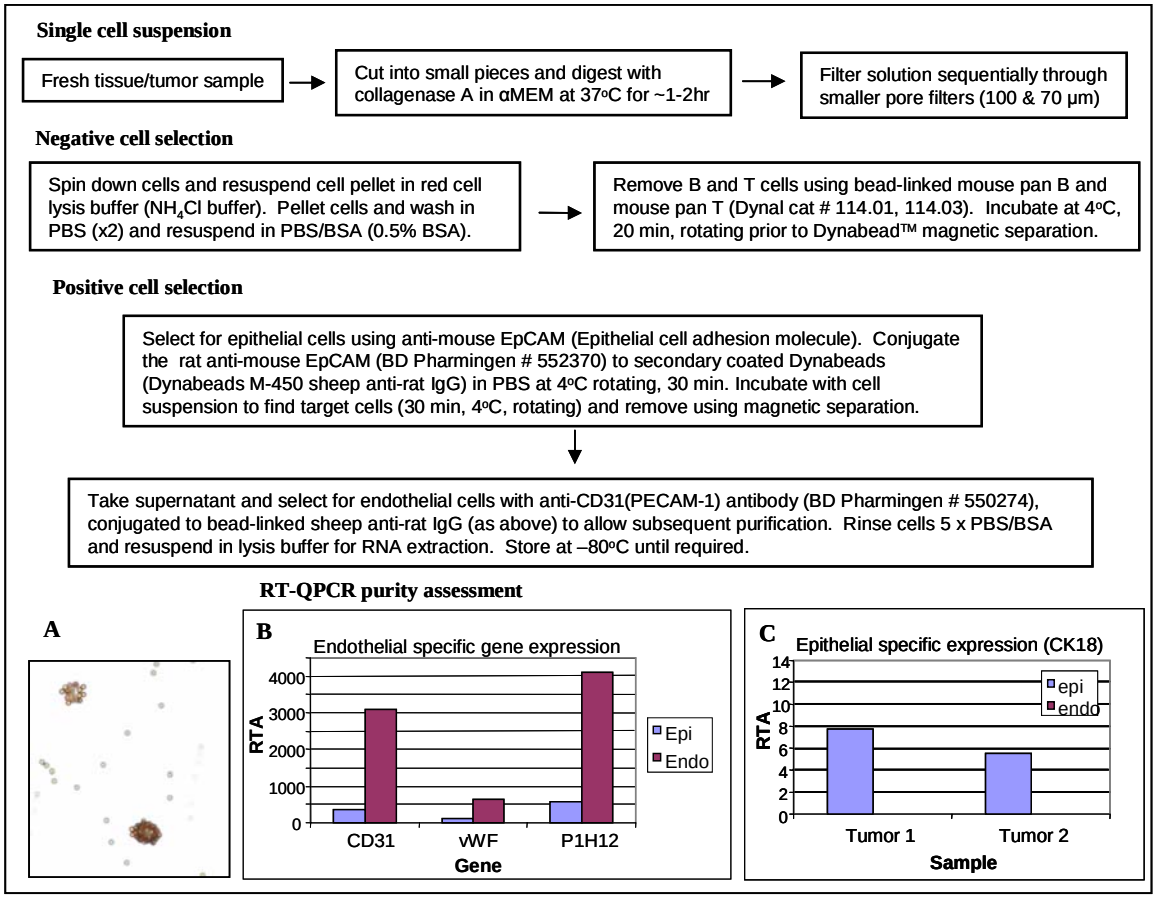

Figure 2: Isolation of endothelial cells from tissues by immunopurification techniques
Bead-bound endothelial cells can be visualized microscopically (A). The purity is confirmed by RT-QPCR of genes specifically expressed in endothelial (B) and epithelial cells (C). The expression of CK18 is absent in the endothelial populations confirming the absence of contaminating epithelial cells

RNA extracted from immunopurified cells (2 samples of 3 pooled replicates) was subjected to two rounds of amplification to yield amplified RNA (aRNA) followed by two step indirect labeling to yield Cy-labelled DNA. Reference samples (new born mouse total RNA) were labelled with Cy3 and test samples (aRNA from epithelial or endothelial cells) were labelled with Cy5. Samples were run on an agarose gel and imaged using the Molecular Imager FX System (BioRad) to ensure quality of labelled cDNA before hybridization to the custom NIA mouse 15K cDNA clone set (containing 15,272 elements, comprising 13,739 unique UniGene identifiers (14)). Arrays were scanned using an Agilent confocal laser scanner (Agilent Technologies, CA) and fluorescence intensities were quantified using GenePix Pro Version 4.1 (Axon Instruments, CA). Genespring version 6 software (Silicon Genetics, CA) was used for analysis, where two biological replicates for each group were normalized using the LOWESS regression model (15). Nonparametric ANOVA and the Benjamini and Hochberg false discovery rate correction was used to identify genes differentially expressed ($p<0.02$) between tumor or endothelial cells derived from highly, weakly and non-metastatic tumors. It should be noted that amplification of RNA did not produce any bias as confirmed by the lack of significant difference between expression profiles of the same sample that was or was not amplified (data not shown).

Gene expression profiles have been obtained from the tumor epithelial and endothelial cells within the primary tumors. For each cell type, a set of genes have been identified whose expression is different between the highly aggressive bone metastasizing lines (4T1.2 and 4T1.13) and the poorly metastatic lines

(66cl4 and 67NR); and in endothelial comparisons also different from that in the normal mammary gland. We have also isolated RNA from the remaining stromal cell component of each of the six primary tumors of each tumor line in the metastasis model in preparation for gene expression profiling of this cell population in future studies.

Primary epithelial changes

Some of the significantly altered genes in highly metastatic 4T1.2 and 4T1.13 tumors (compared to weakly metastatic 67NR and 66cl4 tumors) are listed in Table 1 and Table 1S and 2S (Supplementary Data, Appendix. These include the metastasis suppressor BRMS1 (16, 17) and others involved in development, cell cycle progression, cytoskeletal organization, apoptosis and transformation. Genes involved in the TGFβ pathway were also identified. Of interest was the decreasing expression of BMP4 with increasing metastatic capacity and the reverse response for DACH1. BMP4 is a member of the TGFβ family (18) whereas DACH1 stimulates proliferation and inhibits TGFβ induced apoptosis (19). Given reports that BMP4 can negatively regulate DACH1 expression (20), the down-regulation of BMP-4 may result in the increased expression of DACH1, or conversely, the inhibition of the TGFβ pathway by DACH1 may result in decreased transcription of BMP4. A number of ESTs (summarised in Table 2) were also identified as aberrantly expressed and a selection validated in Task 2.

Of particular interest was the increased expression of the cathepsin inhibitor Stefin A1 in metastatic primary tumors (Table 1). Stefin A1 was enhanced 7.6 fold in highly metastatic 4T1.2 and 4T1.13 primary tumor epithelium compared to tumor cells derived from non- or weakly-metastatic primary tumors.

Primary endothelial alerations

The genes identified aberrantly expressed in highly metastatic tumor-associated endothelium are listed in Table 3 and include, not surprisingly, genes involved in angiogenesis, proliferation, adhesion and motility. Also of interest are some genes whose expression is suppressed in the endothelial cells of the highly metastatic tumors, including two well known tumor suppressor genes, PTEN and LKB1. There are also genes involved in, or regulated by the Hedgehog signalling pathway: Lasp1, CREBBP/EP300 inhibitory protein 1 and FoxP1. Of interest as well are a number of differentially regulated ESTs, shown in Table 5. Interestingly, one EST down-regulated in highly metastatic tumor endothelium has recently been identified as a homolog of large tumor suppressor 2 (LATS2), again revealing endothelial-cell specific decrease in expression of tumor suppressor genes.

2) Profiling expression changes associated with growth in bone

Matched pairs of isolated tumor cells from four 4T1.2 primary tumors and spine metastases were used for Affymetrix microarray analysis. Tumor cells were purified as described above, but with rat anti-mouse Ep-CAM pre-conjugated to sheep anti-rat Dynabeads instead of CELLection Epithelial Enrich, and anti-CD31 for endothelial cell isolation. Immunohistochemistry verified that antibodies against EpCAM and CD31 recognize tumor cells and endothelial cells respectively (Figure 3). Cell purity was confirmed by RT-PCR for epithelial (Ep-CAM, CK18, CK19) and endothelial (CD31, vWF, P1H12, VEGF-R2, Tie2) specific genes (Figure 4). RNA integrity was confirmed by capillary electrophoresis using the Agilent Bioanalyser.

The Affymetrix Two-Cycle Amplification Kit was used to amplify RNA and biotin-labeled RNA (aRNA) was hybridized to Mouse Genome 430 v2.0 microarrays. Array data was analyzed using Genespring GX 7.3 (Agilent Technologies). Gene expression of tumor cells from spine metastases were normalized to their matched primary tumor and an ANOVA (parametric test, not assuming equal variances) was used to identify differentially expressed genes ($p=<0.03$). The top 20 genes (most significantly altered) are shown in Table 4. The majority of these genes were novel genes (ESTs), indicating the potential of this study to identify new genes that have previously not been associated with metastasis. Subsequent to ANOVA, a gene ontology analysis was performed on significantly altered genes to identify groups/pathways that were significantly altered (Table 5). Interestingly, the most significantly altered gene ontology categories were

Description	Common	Function
stefin A1	stfa1	cystatin, cathepsin inhibitor
breast cancer metastasis-suppressor 1	Brms1	Supression of metastasis
ets variant gene 6 (TEL oncogene)	ETV6	cellular aggregation, transformation
complement component 3	C3	up in cancer patients, including highly metastatic human melanoma cells
histidine decarboxylase	Hdc	synthesis of histamine, tumor cell proliferation
SMT3 (supressor of mif two, 3) homolog 1	Smt3h1	protection against TNF etc cell death, cell cycle progression
histidine decarboxylase	Hdc	synthesis of histamine, tumor cell proliferation
dachshund 1 (Drosophila)	DACH1	cell proliferation, inhibits apoptosis (TGFB), developmental gene
bone morphogenetic protein 4	BMP4	member of TGF-beta superfamily, induce cell senescence
topoisomerase (DNA) I	Top1	realxation of supercolied DNA through breakage, cell cycle checkpoint
mitogen activated protein kinase 1	MAPK1	activation of ERK1/ERK2, roles in differentiation
MAP kinase-interacting serine/threonine kinase 2	Mknk2	limit/inhibit translation
developmental pluripotency associated 5	dppa5	development
maternal effect gene	Mater	early development
eomesodermin homolog (Xenopus laevis)	Eomes	early developmental gene
envoplakin	Evpl	cytolinker protein
Rho GTPase activating protein 8	Arhgap8	cytoskeletal organization, cell cycle regulation, ras-mediated transformation
Rho guanine nucleotide exchange factor (GEF) 3	Arhgef3	cytoskeletal rearrangement
ARP3 actin-related protein 3 homolog (yeast)	ARP3	actin nucleation, organization of the cytoskeleton, controls polarised cell growth
heat shock protein 8	HSP8/73	chaperone
autophagy 7-like (S. cerevisiae)	Apg7l	enzyme essential for autophagy
DnaJ (Hsp40) homolog, subfamily B, member 9	Dnajb9	stress induced, induced upon anti-metastatic activity (lung adenocarcinoma cells)
zinc finger protein X-linked	Zfx	inhibits angiogenesis, involved in embryonic growth (sex differentiation)

Table 1 Genes altered in highly metastatic epithelial cells.
Microarray profiling revealed genes that had increased (purple) or decreased (pink) expression in immunopurifed epithelial cells from primary tumors that metastasize to lung and bone.

Microarray ID	p-value	Gene name (accession #)	*Mus Musculus* Protein Name (accession #)	Human Homolog (accession #)
BG077363	0.0020	Breast cancer metastasis-suppressor 1(NM_001037756)	Breast cancer metastasis-suppressor 1-like(NP_001032845)	Breast cancer metastasis-suppressor 1-like(NP_115728)99% identity
BG071250	0.001675	Leucine-rich repeats and calponin homology (CH) domain containing 2, transcript variant 1 (Lrch2), mRNA(XM_204339)	Leucine-rich repeats and calponin homology (CH) domain containing 2 isoform 1 (Lrch2)(XP_204439)	Leucine-rich repeats and calponin homology (CH) domain containing 2(NP_065922)92% identity
BG082965	0.006905	cyclin-dependent kinase 8 (variant 1 and 2-) NM_153599, (NM_181570)	cyclin-dependent kinase 8 isoform a(NP_705827)	CDK8 (AAI04493)98% identity
BG083353	0.001307	RIKEN cDNA 4632434I11 gene, transcript variant 1 (NM_028729)	Hypothetical protein LOC74041 isoform(XP_485962)	Hypothetical protein LOC220042(AAH39268)52% identity
BG066198	0.004408	RIKEN cDNA 2410016F19 gene (NM_026113)	Hypothetical protein LOC67371(NP_080389)	Hypothetical protein LOC112495(NP_612417)75% identity
BG071839	0.00124	EST	/	No homology to human
BG068055	0.009414	EST	/	No homology to human
BG066777	0.005089	*Mus musculus* suppressor of hairy wing homolog 4 (Drosophila), mRNA(BC027163)	Suhw4 protein(AAH27163)	KIAA1584 protein(BAB13410)51% identity
BG066360	0.004154	Rho GTPase activating protein 8(BC024991)	Arhgap8 protein(AAH24991)	proline rich protein 5 isoform 1(NP_851850)88% identity)

Table 2. ESTs with differential expression between highly and weakly metastatic tumours.
Microarray profiling revealed genes that had increased (pink) or decreased (blue) expression in immunopurified epithelial cells from highly metastatic primary tumours that metastasize to lung and bone. Some of the ESTs have now been named and are therefore updated accordingly. The documented metastasis suppressor BRMS1 is also indicated with decreased expression.

Description	Common	Function
endothelial-derived gene	Eg1	angiogenesis
AXL receptor tyrosine kinase	Axl	angiogenesis, cell adhesion and proliferation
cathepsin D	Ctsd	angiogenesis, ECM degradation
macrophage migration inhibitory factor	Mif	angiogenesis, endo growth and migration
ornithine decarboxylase, structural	odc	tumor invasion/angiogenesis/endo proliferation (supression of endostatin)
transducer of ERBB2, 2	Tob2	antiproliferative/inhibits cell cycle progression
H1 histone family, member 0	H1f0	DNA replication/progression through cell cycle
serine/threonine kinase 11	Stk11	tumor suppressor/cell cycle blockage/P53 apoptotic regulation
a disintegrin and metalloprotease domain 8	ADAM8	cell adhesion/growth/osteoclast maturation
RAB20, member RAS oncogene family	Rab20	cell adhesion/migration
integrin beta 1 (fibronectin receptor beta)	Itgb1	cell adhesion/spreading
cell adhesion molecule-related/down-regulated by oncogenes	Cdon	cell adhesion
RAP2B, member of RAS oncogene family	Rap2b	chemotaxis/cell adhesion, morphology, motility/migration
villin 2	Vil2	cytokeleton architecture
LIM and SH3 protein 1	Lasp1	cytoskeleton architecture/cell motility/downstream target of hedgehog
S100 calcium binding protein A9 (calgranulin B)	S100a9	transendothelial migration/adhesion to ECM
phosphatase and tensin homolog	PTEN	tumor suppressor/proliferation/migration
forkhead box P1	Foxp1	growth suppression/transcriptional repressor
suppressor of cytokine signaling 3	Socs3	inhibition of antiproliferative proteins/inhib T cell recognition/osteoclast diff.
BTB and CNC homology 2	Bach2	oxidative stress/reduced proliferation/spontaneous cell death
SWI/SNF related, subfamily a, member 5	Smarca5	decreased expression = cell specific differentiation
Snail homolog 1	Snail	Role in EMT, repression of E-cadherin, over-expressed in cancer
protein tyrosine phosphatase type IVA, member 3	PRL3	Tyrosine phosphatase, expressed in metastatic colorectal cancer

Table 3- Expression profiling of isolated endothelial cells.
Microarray profiling revealed genes that had increased (purple) or decreased (pink) expression in endothelial cells derived from primary tumors that are metastatic (compared to non-metastatic tumors).

those involved in immune response (including defense response and response to biotic stimulus). Additionally, when promoter analysis was carried out on genes that were categorized significant under both ANOVA and gene ontology analysis, it was found that promoter regions specific to binding of interferon regulatory factors was statistically significant. One such interferon regulatory factor (IRF) is IRF-7 and interestingly, this gene is listed as one of the top 20 significantly altered genes (Table 4) and therefore will be followed up for verification and functional analysis.

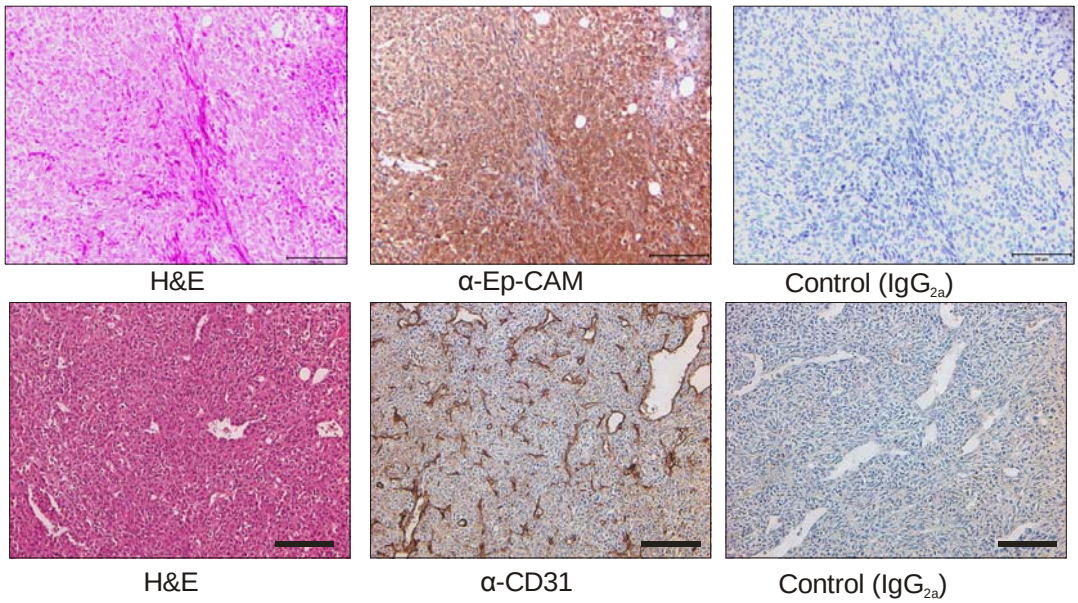

Figure 3: Immunohistochemical staining of Ep-CAM and CD31 on 4T1.2 primary tumor sections. Sections of paraffin embedded 4T1.2 primary tumors were stained with rat anti-mouse Ep-CAM or rat anti-mouse CD31. Signal was then detected with biotinylated goat anti-mouse, conjugation of HRP and then DAB staining (Scale bar = 100µM).

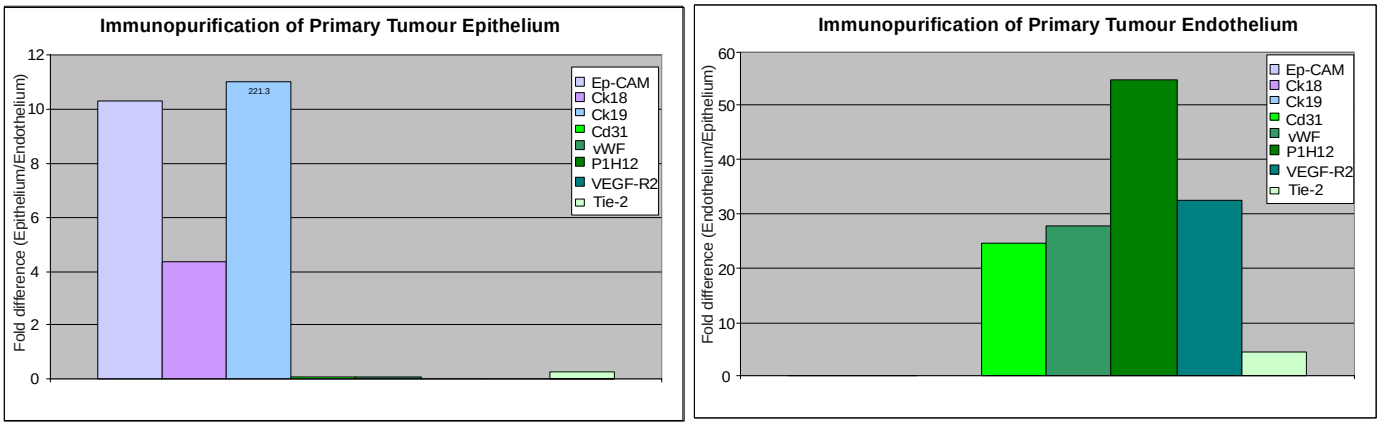

Figure 4: Confirmation of epithelial and endothelial cell purity by realtime RT-PCR
RNA derived from immunopurified cells was reverse transcribed and RT-PCR was then performed using primers specific for epithelial genes (Ep-CAM, Ck18, Ck19) and endothelial genes (Cd31, vWF, P1H12, VEGF-R2, Tie-2). Expression is calculated by CT comparison of the marker gene and GAPDH and then calculating the fold difference between the epithelial and endothelial samples.

Affy ID	p-value	fold change	Gene Name
1438155_x_at	2.83E-06	2.239	BB357373 RIKEN full-length enriched
1418044_at	3.90E-06	1.232	RIKEN cDNA A630042L21 gene
1453312_at	4.08E-06	2.697	BB264725 RIKEN full-length enriched
1450459_at	6.68E-06	0.154	RIKEN cDNA 2010106G01 gene
1416301_a_at	6.75E-06	114.6	early B-cell factor 1
1425588_at	7.31E-06	0.599	602903194F1 NCI_CGAP_Mam3
1422301_at	9.50E-06	0.552	ferritin light chain 1
1440795_x_at	2.14E-05	8.731	BB259371 RIKEN full-length enriched
1456585_x_at	2.26E-05	3.818	BB546892 RIKEN full-length enriched
1428126_a_at	2.27E-05	2.373	RIKEN cDNA 4921506J03 gene
1448810_at	2.67E-05	2.37	glucosamine
1436890_at	2.95E-05	0.248	RIKEN cDNA 5730445F03 gene
1449308_at	3.26E-05	0.0718	complement component 6
1417244_a_at	3.64E-05	0.222	interferon regulatory factor 7
1453977_at	3.70E-05	0.57	SEC8-like 1 (S. cerevisiae)
1428725_at	4.91E-05	0.487	Mus musculus adult male medulla oblongata cDNA
1450821_at	5.02E-05	0.592	p300/CBP-associated factor
1436202_at	5.35E-05	4.955	RIKEN cDNA 2210401K01 gene
1452068_at	5.45E-05	0.624	602890571F1 NCI_CGAP_Lu29

Table 4: Top 20 genes altered in matched spine metastases by significance
P-value generated by ANOVA. Fold change represents primary tumor expression/expression in tumor cells purified from matched spine metastases

Category	Genes in Category	% Genes in Category	Genes in List in Category	% Genes in List in Category	P-Value
GO:6952: defense response	704	3.084	71	6.58	1.50E-09
GO:9607: response to biotic stimulus	716	3.136	71	6.58	3.08E-09
GO:6955: immune response	548	2.401	55	5.097	1.28E-07
GO:42330: taxis	127	0.556	21	1.946	5.23E-07
GO:6935: chemotaxis	127	0.556	21	1.946	5.23E-07
GO:6898: receptor mediated endocytosis	18	0.0789	7	0.649	1.04E-05
GO:50896: response to stimulus	1556	6.816	108	10.01	3.49E-05
GO:50874: organismal physiological process	1320	5.782	94	8.712	4.48E-05
GO:9605: response to external stimulus	512	2.243	45	4.171	5.13E-05
GO:42221: response to chemical stimulus	251	1.1	27	2.502	6.20E-05
GO:9613: response to pest, pathogen or parasite	315	1.38	30	2.78	0.000227
GO:43207: response to external biotic stimulus	323	1.415	30	2.78	0.000349
GO:9628: response to abiotic stimulus	363	1.59	32	2.966	0.000563
GO:6956: complement activation	43	0.188	8	0.741	0.000804
GO:6959: humoral immune response	100	0.438	13	1.205	0.000856
GO:8361: regulation of cell size	106	0.464	13	1.205	0.00148
GO:7585: respiratory gaseous exchange	28	0.123	6	0.556	0.00169
GO:1701: embryonic development (sensu Mammalia)	12	0.0526	4	0.371	0.00181
GO:6954: inflammatory response	149	0.653	16	1.483	0.00187
GO:1558: regulation of cell growth	84	0.368	11	1.019	0.00197

Table 5: Gene ontology analysis of genes significantly altered in spine metastases
Ontology analysis was carried out on genes found to be significantly altered in tumor cells purified from spine metastases when compared to tumor cells derived from matched primary tumors (ANOVA $p<0.005$). Analysis was conducted using Genespring GX 7.3 (Agilent Technologies)

<u>TASK 2:</u> Verify expression of differentially expressed genes found in the mouse model in the relevant cells of human breast tumors, using immunohistochemistry or in situ hybridization (months 9-18).

a. Use realtime RT-PCR and immunohistochemistry in cell culture and in tissue sections of the mouse model to confirm the microarray data (months 9-15).

b. Confirm that these genes are also relevant to breast cancer metastasis to bone in humans by using human tissue arrays to measure expression of the identified genes in the relevant human cell type (endothelial, fibroblast or epithelial) (months 12-18).

Realtime RT-PCR verification

Primary tumor alterations

The differences in expression for several gene candidates has now been confirmed by real time quantitative RT-PCR. From the summary list of epithelial genes altered in highly metastatic primary breast cancer (Table 1), we have compared the expression of BMP4, Dach1 (Figure 5) and Stefin A1 and also 2 ESTs (NM028729 and AK122516- which has know been named LRCH2 (leucine-rich repeats and calponin homology domain containing 2, isoform 1) (Figure 6). Of interest was the decreasing expression of BMP4 with increasing metastatic capacity and the reverse response for Dach1. BMP4 is a member of the TGFβ family, has a role in development, induces senescence and is a negative regulator of Dach1, which stimulates proliferation and inhibits TGFβ induced apoptosis.

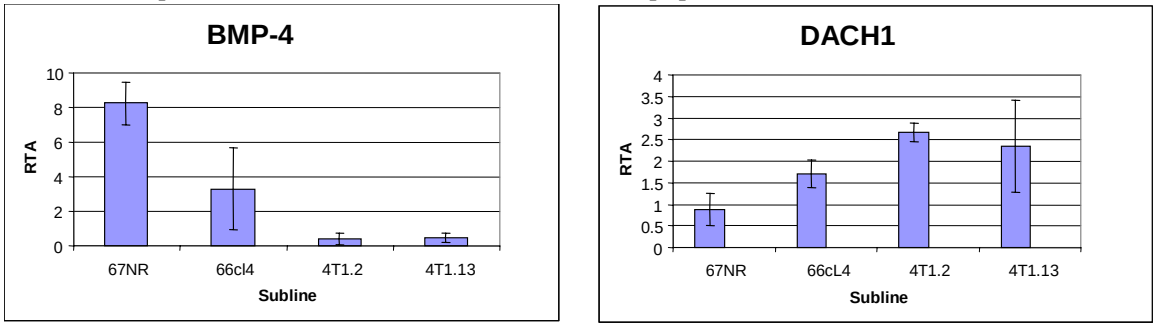

Figure 5 Genes with altered expression in highly metastatic primary epithelium

Genes (BMP-4, DACH1) found differentially expressed by microarray in epithelial cells immunopurified from highly metastatic primary tumors were verified by quantitative RT-PCR. RNA samples from 5 duplicate immunopurified samples from primary tumors of each subline were reverse transcribed using Qiagen Sensiscript RTase. Quantitative RT-PCR was performed using SYBR green and gene specific primers, and GAPDH as a control for normalization. RTA represents the relative transcript abundance when CT values for each gene were normalised to GAPDH. Fold-difference between epithelium derived from high metastatic and low metastatic primary tumors as determined by microarray is indicated below each graph.

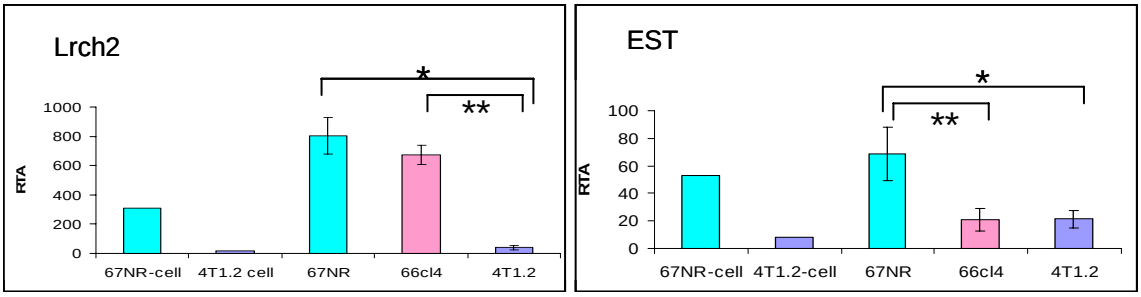

Figure 6. Verification of suppression of EST expression in highly metastatic tumors.

Differential expression of ESTs identified by microarray analysis was confirmed by Real Time RT-PCR analysis using RNA derived from several primary tumours as well as cell line RNA. Expression levels are relative to GAPDH. First two bars (blue 67NR-cell and purple 4T1.2-cell) show RTA from cell line cDNA, all other bars show data from primary tumours. * = P<0.05, ** = P <0.01 Student's t test for comparing primary tumour expression levels.

Stefin A1 (a cathepsin inhibitor) was expressed at much higher levels in the highly metastatic 4T1.2 and 4T1.13 primary tumor epithelium compared to a lack of expression in tumor cells derived from non- or weakly-metastatic primary tumors. This result was confirmed by realtime RT-PCR of RNA from immunopurified epithelial populations derived from the primary tumors (Figure 7A). We also compared

expression of Stefin A1 in immunopurified tumor cells from primary tumors and matched metastases and found that Stefin A was expressed at levels significantly higher in tumor cells from metastases when compared to the matched primary tumor, including lung metastases derived from the weakly metastatic 66cl4 tumor (Figure 7B). Expression was evident only in the context of the tumor microenvironment, with no expression in 4T1.2 and 4T1.13 cells in monoculture (data not shown). Whilst there is a single Stefin A homolog in humans, three homologs exist in the mouse (A1, A2 and A3). Since only Stefin A1 was present on the custom 15K array, we used primers that distinguish between Stefin A1, A2 and A3 and real time RT-PCR, to confirm that all homologs are induced in highly metastatic primary tumors (Figure 7C). These results suggest that Stefin A has potential as a prognostic marker to predict distant metastases. Affymetrix microarray comparison of Stefin A1 and A3 (A2 was not present on the array) expression in purified 4T1.2 tumour cells from primary tumors and matched spine metastases is consistent with real time RT-PCR findings, with Stefin A expression being much higher in metastases in all four biological replicates as indicated by the heatmap (Figure 7D).

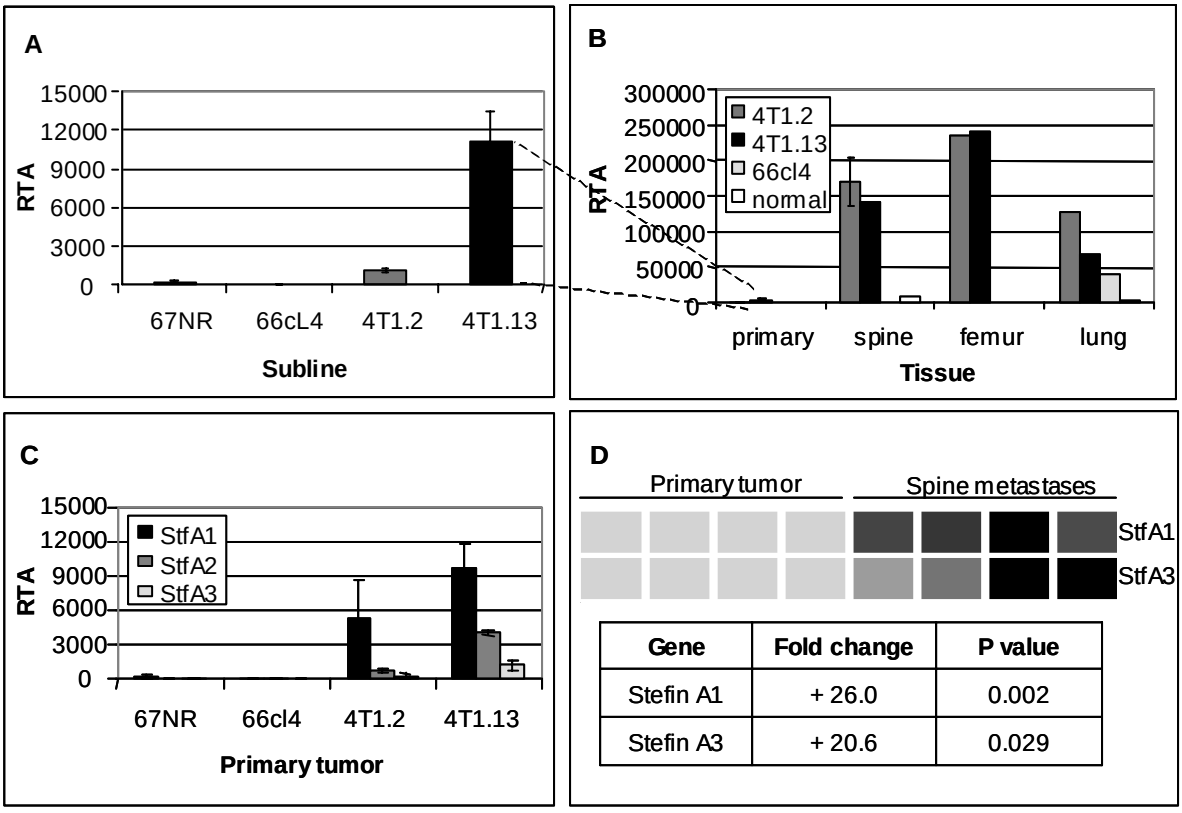

Gene	Fold change	P value
Stefin A1	+ 26.0	0.002
Stefin A3	+ 20.6	0.029

Figure 7 Stefin A transcript expression in primary tumors and metastases
RNA isolated from tumor cells derived from primary tumors (A) and matched metastases (B) were reverse transcribed and real-time RT-PCR was used to detect Stefin A1 expression relative to GAPDH. C) Expression of the three murine Stefin A homologs in RNA extracted from whole primary tumors. D) Microarray comparison of Stefin A1 and A3 expression in four replicate samples of tumor cells purified from primary and matched spine metastases. Signal intensity in spine metastases was normalized to matched primary samples.

We have also verified the microarray data derived from primary tumor vascular endothelium (Table 3), before proceeding to a study of the expression of the genes *in situ* in tumors. Aberrant expression of FoxP1, LKB1, MIF, LATS2 and Snail in vascular endothelium of highly metastatic primary tumors has now been verified by real time quantitative RT-PCR. (Figure 8). With increasing metastatic capacity,

endothelial expression of FoxP1, LKB-1 and LATS2 decreased. On the other hand, there was a trend toward increased expression of MIF in the endothelium of highly metastatic 4T1.2 tumors.

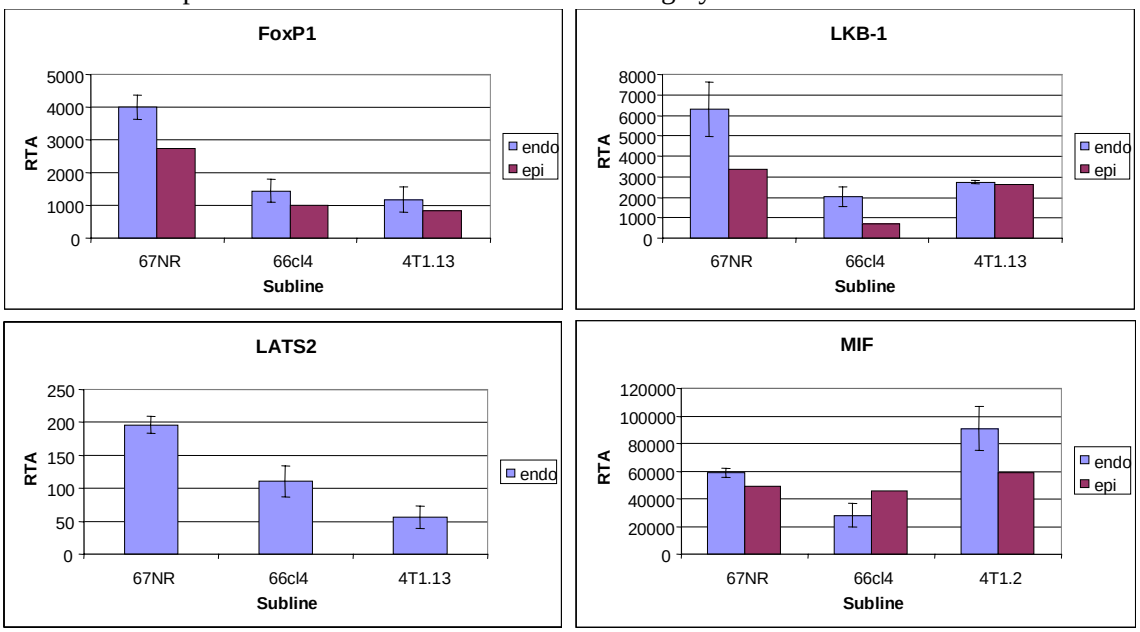

Figure 8. Genes with altered expression in highly metastatic primary endothelium
FoxP1, LKB1, MIF and LATS2 found to be differentially expressed in endothelial cells immunopurified from highly metastatic primary tumors, were verified by quantitative RT-PCR. RNA samples from 5 duplicate immunopurified samples from primary tumors of each subline were reverse transcribed and RT-PCR amplified using primers specific to genes of interest.

We have also performed verification studies on two genes found upregulated in highly metastatic primary tumor endothelial cells, Snail and PRL-3.

Snail and PRL-3 were originally identified in recent work on gene expression changes in vascular endothelium associated with human invasive breast cancer (13). As these two genes were not included on our mouse 15k array, I used quantitative RT-PCR to investigate whether these genes are expressed in primary tumors in our model and, if so, whether the expression was altered in highly metastatic tumors. Studies using RNA derived from immunopurified epithelial and endothelial cells isolated from non-metastatic (67NR), weakly metastatic (66cl4) and highly metastatic (4T1.2, 4T1.13) primary tumors showed a similar expression pattern as seen in human cancer, yet revealed additional information regarding their regulation during metastasis. PRL-3 was expressed solely in the vascular endothelium of invasive breast cancer in humans, with no expression observed in the tumor epithelium (Figure 9A). This was also seen in the murine model, with expression only obverved in the purified tumor endothelium (Figure 9B). Interestingly, the expression of PRL-3 increased in the endothelial cells derived from highly metastatic tumors indicating a possible role in metastasis. Snail was expressed in both the tumor epithelial cells and associated endothelium in invasive breast cancer (Figure 9A). Again, this was seen in the murine model, with both epithelial and endothelial cell populations expressing Snail. As with PRL-3 there was an enhanced expression of Snail with metastasis and this was specific to the endothelial cells, resulting in much greater endothelial expression of Snail in the highly metastatic primary tumors (Figure 9C).

Bone metastases

Selected genes identified in task 1 as altered in spine metastases when compared to matched primary tumors have been verified in purified tumor cells using realtime PCR. These include the metastasis suppressed genes, interferon regulatory factor 7 (IRF7) (Figure 10) and the interleukin receptors IL13rα1

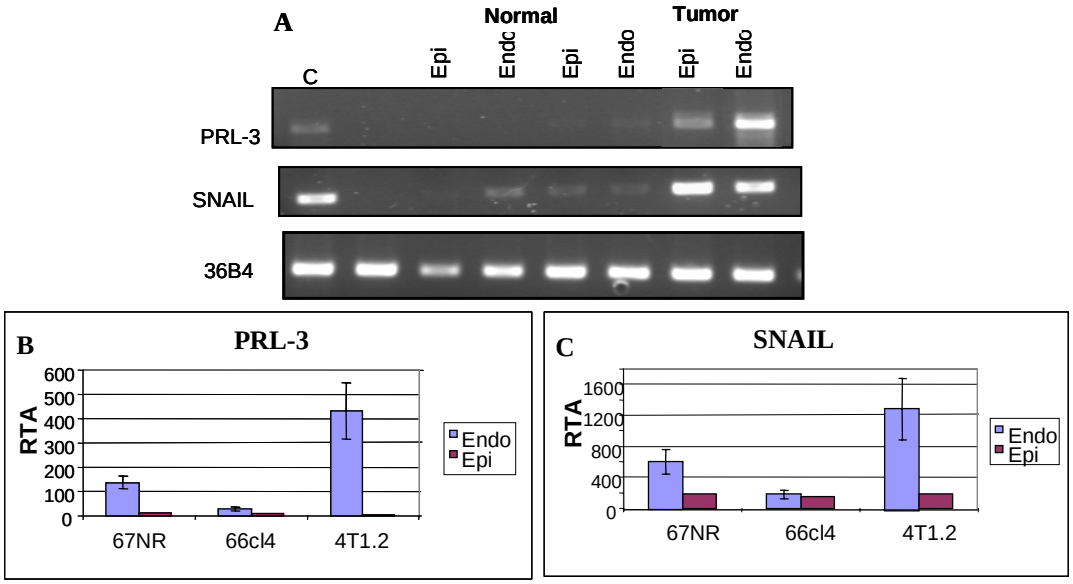

Figure 9 Comparison of endothelial expression of PRL-3 and Snail in human and murine breast cancer
A) Human RNA expression (RT-PCR) of PRL-3 and Snail in epithelial and endothelial cell populations immunopurified from normal mammoplasty tissue or from freshly resected invasive breast cancer samples. Similar expression patterns for PRL-3 and Snail were detected by quantitative RT-PCR in epithelial and endothelial cells immunopurified from primary tumors from the murine model (B,C). The use of primary tumors with varying metastatic potential also revealed the increase in expression of both genes in endothelium derived from highly metastatic 4T1.2 tumors.

and IL4rα (Figure 11). These two interleukin receptors were significantly suppressed in bone metastases and are known targets of IRF7. Other genes verified include the chemokine ligands CCL7 and CXCL16 (Figure 11), both of which were also suppressed in matched metastases compared to expression in the primary tumor.

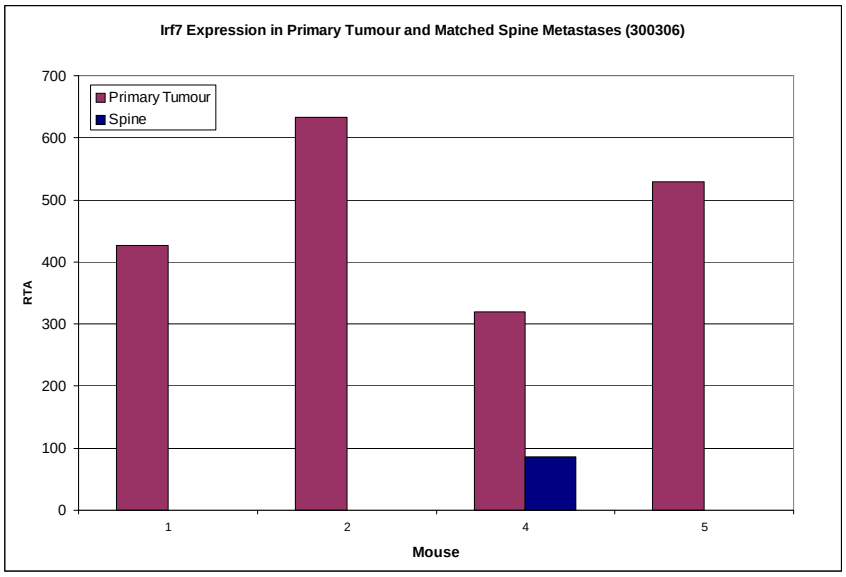

Figure 10. Expression of IRF7 in primary tumors and spine metastases
RNA extracted from epithelial cells immunopurified from 4T1.2 primary tumors and matched metastases was reverse transcribed and realtime RT-PCR was used to detect IRF7 expression.

In situ hybridisation

We have optimised an *in situ* hybridisation technique to verify cell specific candidate gene expression in tissues derived from the model. This technique is utilised when antibodies recognising the candidate

proteins are not available, with some anti-human antibodies available but a lack of those that recognise murine antigens. The method involved generation of a cocktail of riboprobes spanning gene transcripts (designed across intron/exon junctions). Riboprobes were generated by end-labelling 5' and 3' ends of PCR primers with T7 and SP6 promoter sequences and PCR amplification of DNA sequences of interest followed by *in vitro* transcription using T7 and SP6 polymerase, generating sense and anti-sense probes respectively. The *in vitro* transcription includes labelling of transcripts with FITC. Paraffin embedded sections of 67NR, 66cl4, 4T1.2 and 4T1.13 primary mammary tumors and their corresponding metastases (see Figure 1) were used for *in situ* hybridisation (ISH). Protocols were modified from those previously described (13, 21), including deparaffinization and fixation of tissues, pre-treatment for access to target nucleic acid sequence and riboprobe hybridization overnight, with the use of FITC riboprobe labelling replacing DIG as previously used. Riboprobe/FITC signal was detected and amplified using the GenPoint™ Fluorescein Tyramide Signal Amplification System (DakoCytomation). The signal was visualized using DAB staining followed by nuclear counter staining with hematoxylin.

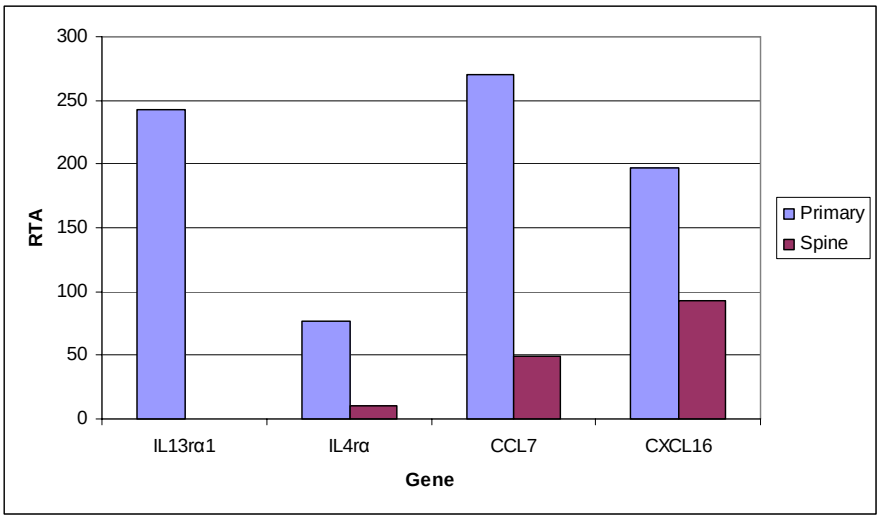

Figure 11. Realtime RT-PCR verification of genes suppressed in spine metastases
RNA extracted from epithelial cells immunopurified from 4T1.2 primary tumors and matched metastases was reverse transcribed and realtime RT-PCR was used to detect IL13rα1, IL4rα, CCL7 and CXC16 expression.

Stefin A1
Using *in situ* hybridisation, the increased expression of Stefin A1 throughout metastatic progression was verified histologically. As a positive control, mouse embryos were stained to reveal positive cells within the liver at day 15.5. By staining sections from primary mammary tumors, expression (positive staining) was observed in only the highly metastatic 4T1.2 and 4T1.13 tumors, and such expression was limited to only specific subsets of tumor cells (Figure 12). In contrast, sections from matched lung metastases revealed staining of metastatic lesions that appeared in a large proportion of tumor cells (Figure 12). This supports the hypothesis that the higher levels of expression observed in metastatic lesions compared to primary tumors detected by quantitative RT-PCR was due to only a subset of cells in the primary tumor expressing the gene and either a selection of these cells that metastasise and grow in distant sites, or induction of stefin A1 in tumor cells once they reached the microenvironment of the lung or bone. As Stefin A is only a small gene (290 bp), only one probe could be used for ISH detection and we usually use at least 2 probes that span the gene, each being ~500 bases long. This resulted in staining that was less intense than is preferable. Chemicon now has an anti-mouse Stefin A antibody that we used for immunohistochemistry (see below).

Snail
As stated above, snail was originally identified in recent work on gene expression changes in vascular endothelium associated with human invasive breast cancer (13). In our model, realtime-PCR has revealed enhanced expression of Snail with metastasis is specific to the endothelial cells, resulting in much greater endothelial expression of Snail in the highly metastatic primary tumors such that it could be detected by

in situ hybridisation (Figure 13). We are now looking at the functional effects of altering the expression of the snail in primary endothelial cells to determine the effect on endothelial growth and interactions with tumor cells in culture.

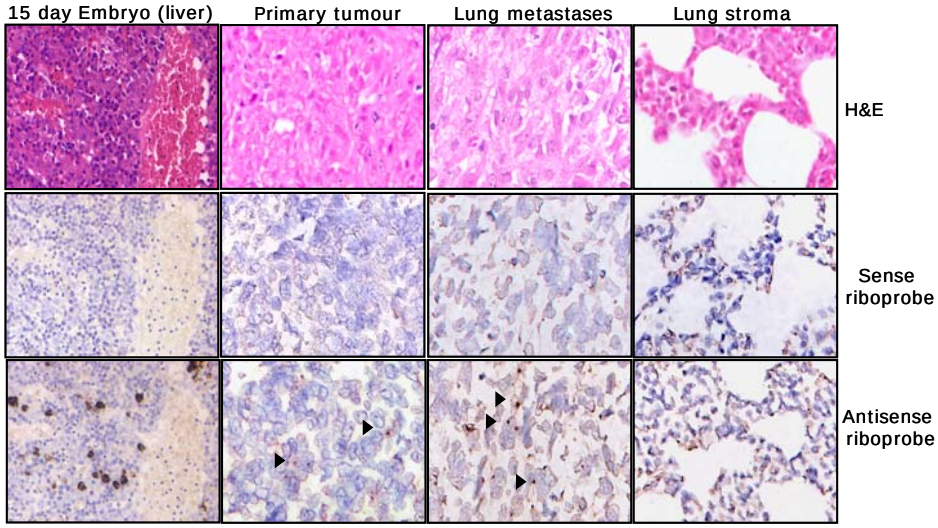

Figure 12 Expression of Stefin A1 (Stfa1) in primary and metastatic tumors.
Expression of Stefin A1 was validated by *in situ* hybridisation. 4T1.2 primary tumors and lung metastases were stained with stefin A1 antisense riboprobes and sense probes as controls. Riboprobes were FITC labelled and detected using anti-FITC HRP followed by DAB staining and counter staining with hematoxylin. Tumor staining (brown) is indicated by arrows. Mouse embryo (15.5 days) was stained as a positive control and staining was detected in the liver.

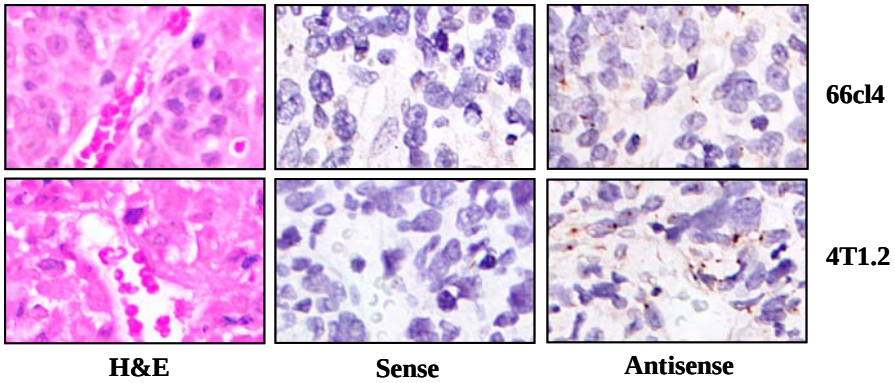

Figure 13 Verification of Snail expression by in situ hybridisation
The increase in endothelial expression of Snail (seen in Figure 9) was detected by ISH, with binding of the anti-sense cocktail of riboprobes (as indicated by brown staining) and absence of staining in sense controls.

Laminin α5
We have used the optimised *in situ* technique to verify expression of the extracellular matrix protein LNα5 in highly metastatic primary tumors. Using mouse embryo as a positive contol, as expected LNα5 was expressed in the sub-epidermal layer of the skin (Figure 14). In primary tumors, only the highly metastatic 4T1.2 tumor cells expressed the gene, verifying it's possible role in breast cancer metastasis.

Immunohistochemistry-mouse and human tissues
Stefin A
To verify protein expression in the murine model, normal mammary gland and 67NR, 66cl4, 4T1.2 and 4T1.13 primary tumors were analysed for presence of Stefin A using an antibody targetting the N-terminal region that recognizes all three homologs. By immunohistochemistry, we detected Stefin A only in the metastatic 4T1.2 and 4T1.13 primary tumors (Figure 15). Expression was higher at the periphery of the

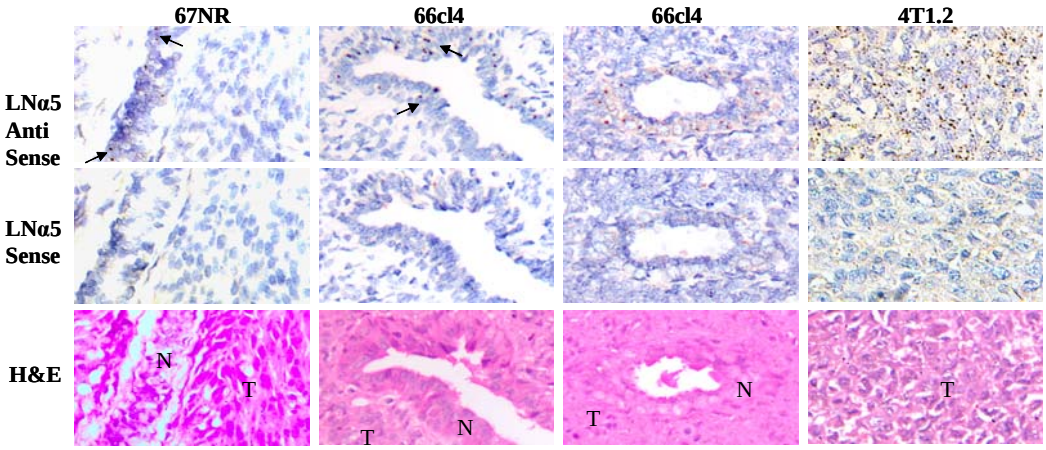

Figure 14 Expression of Laminin α5 (LNα5) in primary tumors.
Expression of LNα5 was validated by *in situ* hybridisation. 67NR, 66cl4 and 4T1.2 primary tumors were stained with a cocktail of LNα5 antisense riboprobes and sense probes as controls. Riboprobes were FITC labelled and detected using anti-FITC HRP followed by DAB staining and counter staining with hematoxylin. Tumor staining is visualised in brown.

tumor, in contact with surrounding stroma. This was also the case in matched lung and bone metastases, where Stefin A was localized predominantly in tumor cells interacting with stroma (Figure 15). In tumor-bearing spines, but not in normal spine, scattered inflammatory cells in regions adjacent to the tumor were positive for Stefin A (Figure 15).

To determine the clinical relevance of Stefin A as a marker of metastasis, we analysed expression in human tissues. In normal reduction mammoplasty tissue, Stefin A was frequently expressed in the myoepithelial layer surrounding normal ducts and lobules (Figure 16A). The luminal epithelium, from which the majority breast tumors arise, was negative in numerous normal breast tissue samples from different individuals. In contrast, a subset of primary tumors expressed Stefin A (Figure 16B, C). Since the murine studies revealed increased Stefin A expression in lung and bone metastases, human lung and bone metastases were also analysed. As in our murine model, tumor deposits in lung (Figure 16D) and bone (Figure 16E, F) expressed high levels of Stefin A. Again, the strongest staining was in tumor deposits that were interacting with the lung or bone stroma. In regions of lung metastases where cells were not in contact with stromal cells, Stefin A was not expressed (data not shown).
A small cohort of primary tumors (n=25) from patients with known outcome was used to investigate the prognostic significance of Stefin A. Primary tumors that formed metastases in lung or bone expressed Stefin A with much higher frequency than non-metastatic primary tumors (Figure 16). This was indicated by univariate disease-free survival (DFS) analysis that showed a significant correlation between improved outcome and lack of Stefin A tumor expression (p=0.017)(Figure 16G). Although a trend was observed between Stefin A expression and risk of cancer-related death, this relationship was not significant (p=0.087) due to the small sample size (Figure H). We have also stained and scored a large cohort (>200 patient samples) of primary breast tumors from the Garvan Insititute, Sydney and we are waiting for final analysis. Preliminary analysis, however, has shown that Stefin A expression does correlate with increased risk of metastatic recurrence (Logrank (Mantel-Cox) test, p= 0.0002), yet this only represents a subpopulation of Stefin A positive tumors and will be updated upon completion of analysis.

IRF7
We have optimised the use of an anti-mouse IRF7 antibody that had previously not been used for immunohistochemistry, to verify the suppression of IRF7 in bone metastases. We found that IRF7 is extensively expressed in tumor cells of 4T1.2 primary tumors (Figure 17). In contrast, tumor cells within matched bone metastases had lost expression of this protein (Figure 17), verifying Affymetrix microarray

and realtime RT-PCR results. We will now be staining multiple matched primary tumors and metastases to determine whether the loss is specific to bone metastasis or whether there is also suppression in other metastases, such as lung.

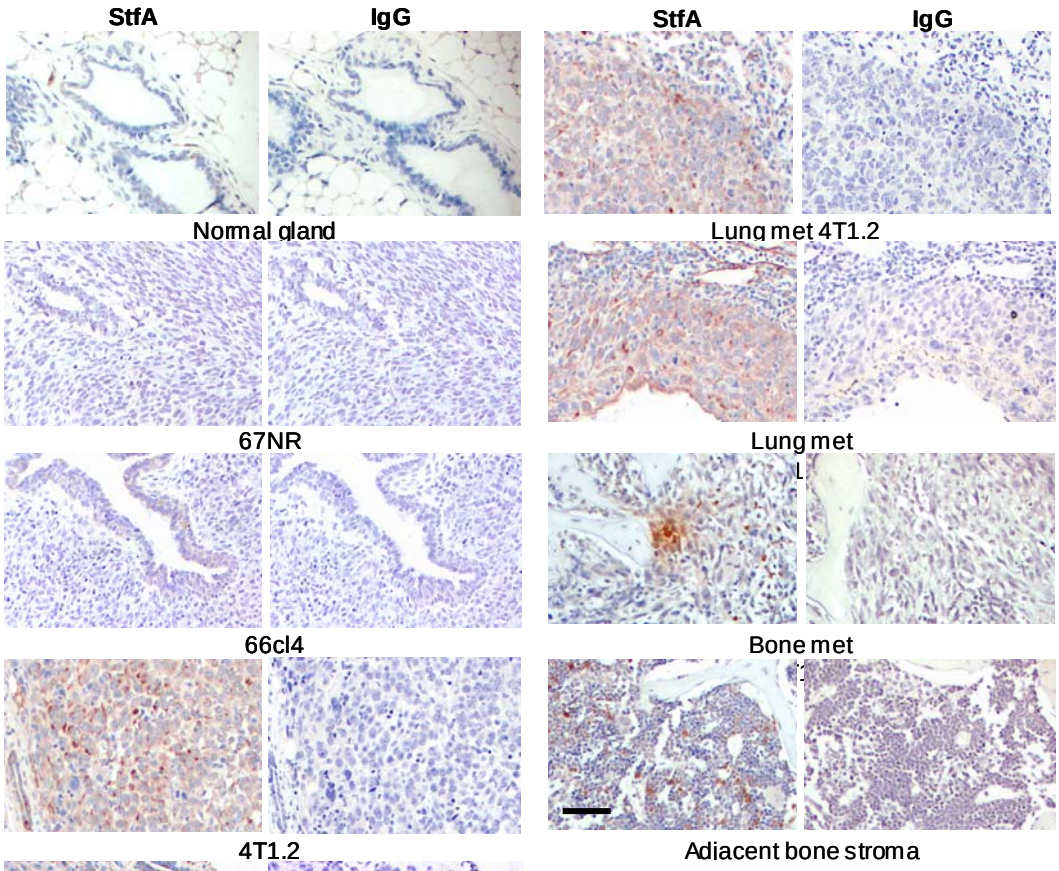

Figure 15 Immunohistochemistry of Stefin A expression in the mouse model

Stefin A protein expression in normal mammary fat pad, 67NR, 66cl4, 4T1.2, and 4T1.13 primary tumors, and in lung and spine metastases from 4T1.2 and 4T1.13 tumor bearing mice. Stefin A was detected with rat anti-mouse Stefin A, with rat IgG_2 as an isotype control and visualized with DAB. All tissues were counterstained with hematoxylin. Scale bar represents 50 μm.

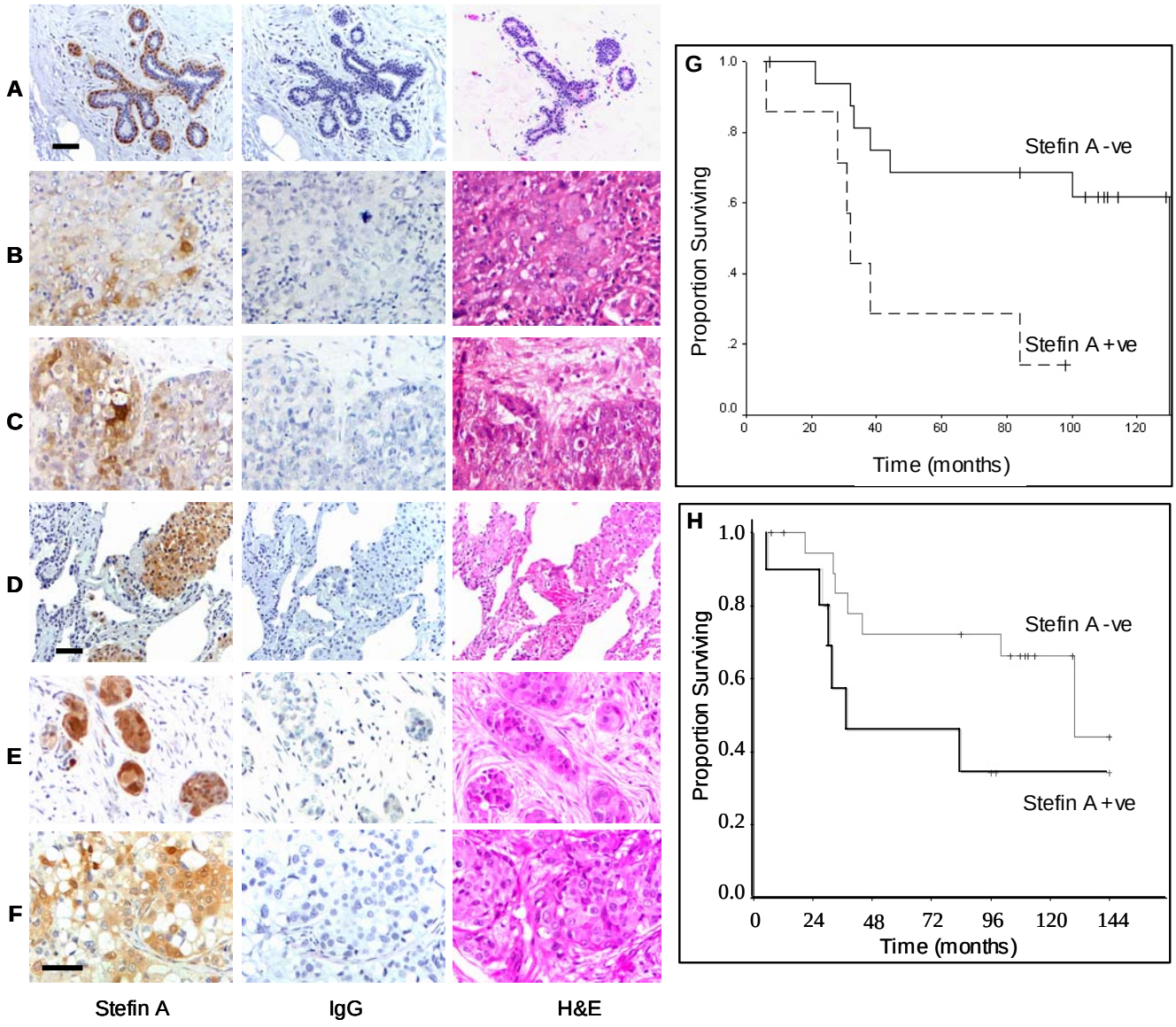

Figure16 Immunohistochemistry of Stefin A expression in human tissues
Sections of formalin fixed, paraffin embedded reduction mammoplasty tissue (A), primary breast tumors (B,C), or metastases in lung (D) and bone (E,F) were stained with mouse anti-human Stefin A or 1B5 hybridoma supernatant control and visualized with DAB. All tissues were counterstained with hematoxylin. Scale bar represents 50 μm. Kaplan-Meier survival curve comparing disease free survival (G) or death due to disease (H) in patients expressing Stefin A and patients lacking Stefin A expression in the primary tumor. Stefin A expression was measured in primary breast tumor tissues from a cohort of 25 patients with known outcome.

TASK 3 In vitro functional analysis of the selected candidates (months 18-36).

a. Perform *in vitro* invasion and migration assays using tumor cells co-cultured with endothelial cells or fibroblasts isolated from primary tumors with known metastatic potential (months 18-24).
b. Generate endothelial cells or fibroblasts transiently infected with a retrovirus expressing a cDNA construct for one of the genes of interest. Use these cells in the invasion and migration assays described above with tumor cells of varying invasive potential (months 18-36).

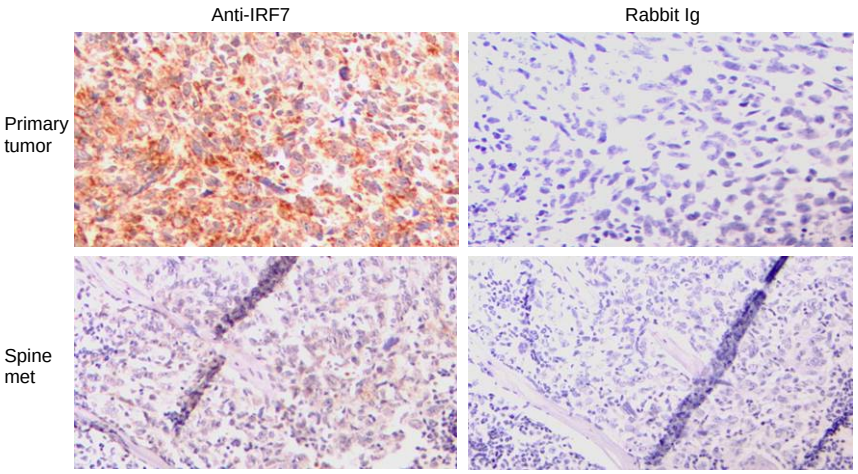

Figure 17. Expression of IRF7 in primary tumors and spine metastases.
Sections of paraffin embedded tumors were stained with rabbit anti-mouse IRF-7 or rabbit Ig as a control. T indicates a tumor within the spine.

Stefin A

Due to the impact of the microenvironment on Stefin A expression, we decided to investigate the induction of Stefin A in co-cultures *in vitro*. Expression is evident only in the context of the tumor microenvironment, with no expression in 4T1.2 and 4T1.13 cells in monoculture. We wanted to determine whether we could stimulate the expression of Stefin A in these cells when co-cultured with stromal cells *in vitro* to investigate the effect of the surrounding microenvironment. We were able to induce Stefin A to modest levels in co-cultures of 4T1.2 cells with mammary gland stromal cells (Figure 18, summarized below) and also with primary mammary fibroblasts and ECM components, however expression was lower than that observed *in vivo* and may indicate additional factors that are required to induce Stefin A. Stromal cells were isolated from mammary fat pads and cultured either alone, or in contact with tumor cells. When co-cultured with the non-metastatic 67NR cells or weakly metastatic 66cl4 cells there was no induction of Stefin A1 expression. Interestingly, when the highly metastatic 4T1.2 cells were co-cultured with the fatpad stroma, an significant induction in expression was observed by quantitative RT-PCR (Figure 18). This effect was not observed when cells were cultured together in transwell inserts (and therefore not in contact) indicting a requirement of cell-cell contact for induction of Stefin A1 expression. Even though it can be hypothesised that cathepsins may be involved in Stefin A1 induction, there was no significant difference in expression of cathepsin B, S, K and C with co-cultures

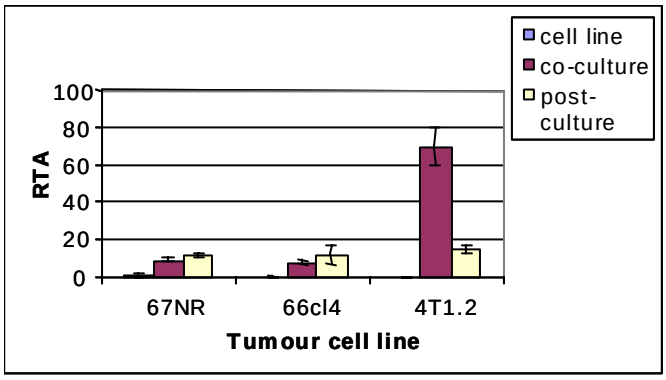

Figure 18 Co-culture induction of Stefin A1
Mammary fat pads were resected and collagenase A digested into single cell suspensions. Filtered cells were then plated and allowed to attach overnight. For contact co-cultures tumor cells (67NR, 66cl4 or 4T1.2) were then added to stromal populations (co) or cultured separately (cell line) overnight in serum-free media. Post-culture represents cells that were incubated separately and then mixed in lysis buffer to determine the additive expression of Stefin A1 in tumor and stromal cells when not cultured together. Expression was detected using quantitative RT-PCR of Stefin A1 and a comparison to GAPDH.

(Figure 19). However, there were some differences, including the enhanced expression of cathepsin L only in co-cultures with 4T1.2 cells and cathepsin C was only expressed in 4T1.2 cells, with a lack of expression in 67NR and 66cl4 cells cultured alone.

It remains to be investigated whether there are changes in the activity of specific cathepsins, that may subsequently lead to Stefin A1 expression as a mechanism of inhibition. We are now investigating the possible mode of Stefin A1 induction, including the role of cathepsins (since Stefin A1 is an intracellular

inhibitor of cathepsins) and whether stromal cells isolated from other organs (tissues that have metastatic growth in the 4T1.2 model and those that do not develop any tumor burden after primary tumor formation) can also induce Stefin A1 expression upon contact co-culture. Due to the difficulty we have faced so far inducing Stefin A expression in cells in culture to levels in the range of that seen in culture, we may need to functionally dissect the role of cathepsins and their inhibitor Stefin A using *in vivo* studies.

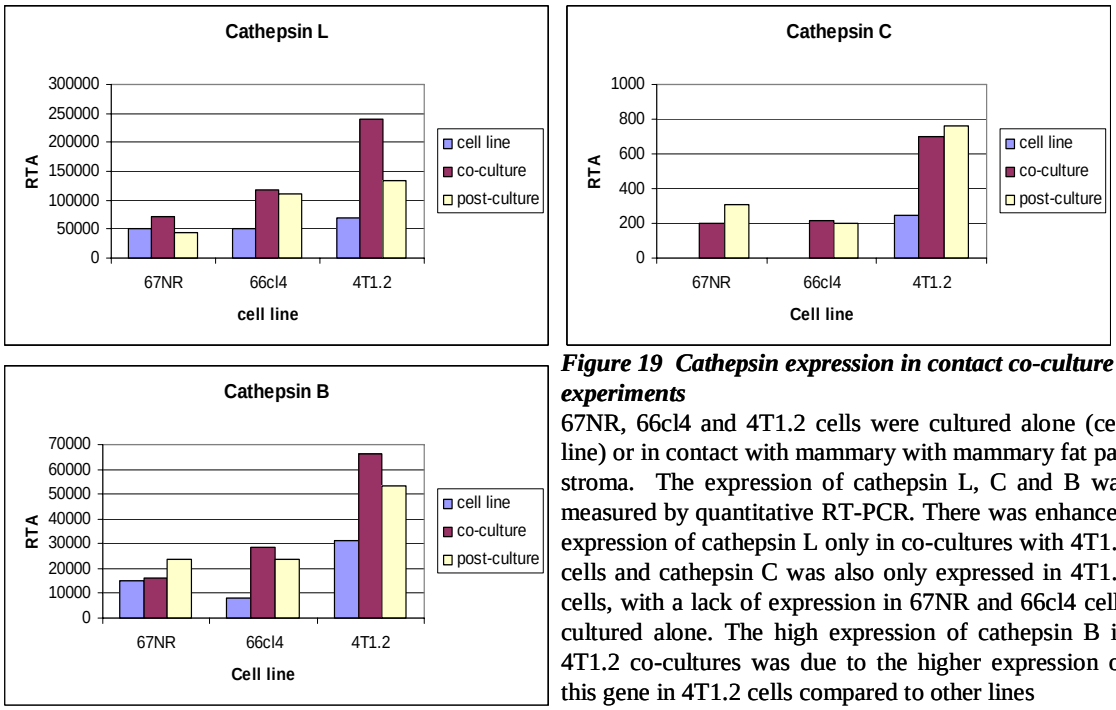

Figure 19 Cathepsin expression in contact co-culture experiments

67NR, 66cl4 and 4T1.2 cells were cultured alone (cell line) or in contact with mammary with mammary fat pad stroma. The expression of cathepsin L, C and B was measured by quantitative RT-PCR. There was enhanced expression of cathepsin L only in co-cultures with 4T1.2 cells and cathepsin C was also only expressed in 4T1.2 cells, with a lack of expression in 67NR and 66cl4 cells cultured alone. The high expression of cathepsin B in 4T1.2 co-cultures was due to the higher expression of this gene in 4T1.2 cells compared to other lines

ESTs (Potential Metastasis Suppressors)

The two ESTs that were verified by realtime RT-PCR as genes suppressed in highly metastatic primary tumors, and hence potential metastasis supressors, were studied for their function *in vitro*. LRCH2 (1.7 Kb) and EST (2.8 Kb) have been cloned into retroviral vectors, tranfected into viral packaging cells (phoenix) and infected into 4T1.2 cells to generated stable over-expression lines. We have overexpressed C- and N-terminal flag tagged and untagged constructs to ensure that the location of the Flag tag does not interfere with protein function or localisation in the cell. The Flag-tagged proteins were generated to allow detection of the expressed proteins, since antibodies against Lrch2 and EST do not exist.

The processes of proliferation, migration, invasion, adhesion, and angiogenesis are all critical for the formation of distant metastasis. Therefore, we determined whether the 4T1.2neo1 cell lines with expression of EST and Lrch2 differed in these metastasis-related processes from 4T1.2neo1 cells containing the base vector. In order to determine this, functional *in vitro* assays were completed such as proliferation, migration, and invasion assays.

Proliferation: The proliferation rate of each modified cell line was compared to the rate of the base vector cells. Cells were counted in duplicate every day, for 6 days. We hypothesized that the expression of EST or Lrch2 has an impact only on metastases and not on the primary tumour growth. Therefore we expected that the proliferation rate for each cell line would remain unchanged after over-expression of the EST or Lrch2. Figure 20 shows that all cell lines have similar proliferation rates, no difference was seen with the control 4T1.2pBABE cells.

Migration: Chemotactic migration of tumour lines towards an attractant was determined using a Transwell migration assay. The extent of migration of Lrch2 Flag Fwd, EST Flag Rev, EST and the base vector expressing cells in response to 5% serum as the chemoattractant was measured by the number of cells that were able to cross from the basal surface, through pores within the membrane of the insert, to the lateral

surface. There was a significantly reduced number of migrated cells in the 4T1.2neo1/EST cells when compared to the base vector (P<0.01). The other transformed cell lines, Lrch2 Flag Fwd and EST Flag Rev, did not show any reduction in the ability to migrate (Figure 21). We need to determine whether the phenotype observed with the EST expression line is maintained after single cell cloning and also whether the flag-tagged contruct has an altered cellular localisation to explain the effect observed only in cells stably expressing the untagged construct.

Invasion: The invasive capacity of the tumour lines (pBABE, Lrch2 Flag Fwd, EST Flag Rev, and EST) was examined by their ability to invade through a Matrigel barrier in response to 5% serum as chemoattractant. Again, expression of the untagged EST reduced the number of cells with an ability to invade compared to the base vector (P<0.05). The other cell lines, Lrch2 Flag Fwd and EST Flag Rev, did not show any reduction in the ability to migrate (Figure 22). This cell line has reduced invasion and migration and therefore we will be investigating this further as stated above (in migration results).

It is important to note that *in vitro* functional assays do not represent every step involved in metastasis *in vivo*. Therefore, regardless of whether a phenotype is observed in *in vitro* assays, it is more biologically relevant to investigate the functional role of genes *in vivo*.

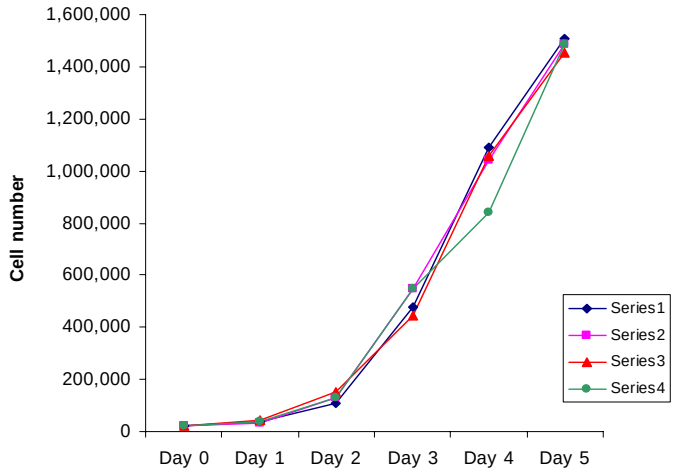

Figure 20. Proliferation assay. Cells were plated (20.000) on day 0. Cells were counted in duplicate every day. Each data point is an average of two counts. Similar proliferation rates were seen for each cell line.

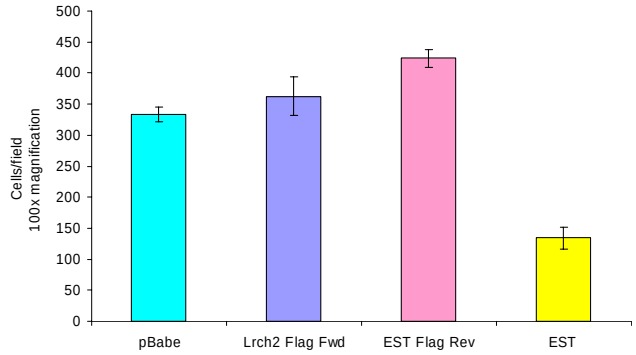

Figure 21. Migration assay.
Migration assay was carried out in Transwells for Lrch2 Flag Fwd, EST Flag Rev, EST, and base vector in response to 5% serum. After 4-6 hours, the number of cells traversing the membrane was counted. One 100x magnification field was counted per sample. Statistical differences were detected for EST compared to base vector *, P <0.01, using the Student's t test for base vector compared with transformed cell lines.

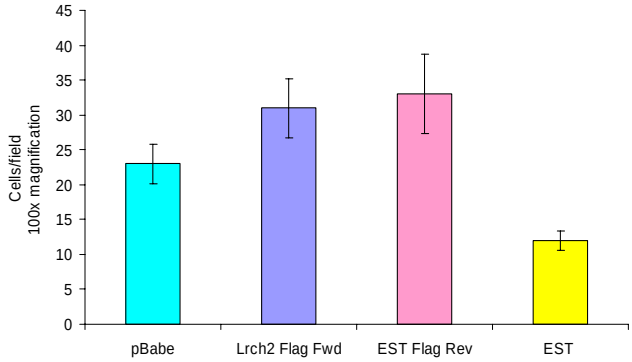

Figure 22. Invasion Assay
Invasion through Matrigel was carried out in Transwells for Lrch2 Flag Fwd, EST Flag Rev, EST, and base vector in response to 5% serum. After overnight incubation, the number of cells traversing the membrane was counted. One 100x magnification field was counted per sample. Significantly difference between EST and base vector *, P<0.05

.

TASK 4: Explore the function of the selected genes in metastasis in vivo (months 18-36).

a. If available, obtain mice null for the stromal gene of interest. Backcross onto a Balb/c background (months 18-30).
b. Measure the metastatic capacity of the bone metastasizing clone in mice lacking the relevant stromal gene (months 30-36).
c. In normal Balb/c mice, use neutralizing antibodies, an antagonist or a small molecule inhibitor of the gene if interest to measure the effect on bone metastasis (months 18-36).

Stefin A and Cathepsin Proteases

It was of interest to determine whether enhancing the expression of Stefin A1 in 4T1.2neo1 cells *in vitro* would alter the metastatic burden when cells were injected into the mammary fat pad. Stefin A1 was cloned into the pBabe vector (containing a puromycin resistance gene) and transfected into the phoenix viral packaging line. The 4T1.2 cells were then infected with virus either containing the pBabe base vector (BV, as a control) or the pBabe-Stefin A1 plasmid and stably selected by growth in puromycin. Expression was confirmed by quantitative RT-PCR (Figure 23) and high expressers were pooled for *in vivo* studies.

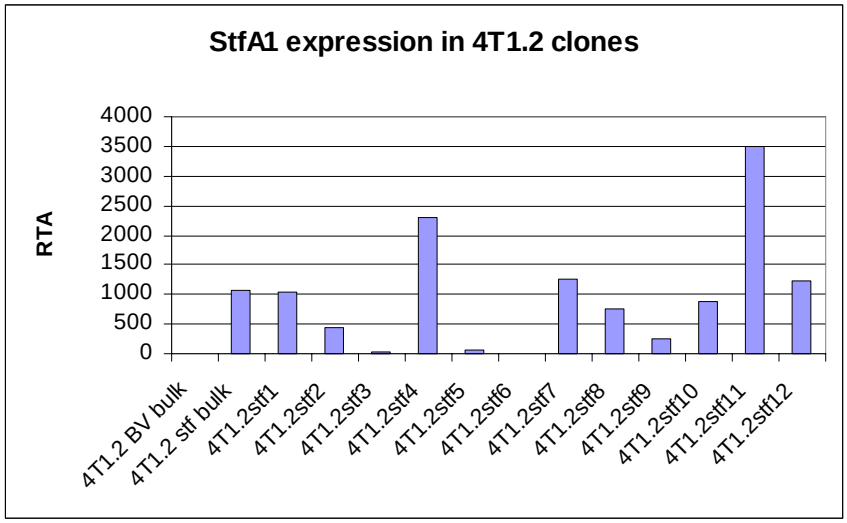

Figure 23 Stefin A1 over-expression in 4T1.2 cells does not effect primary tumor growth in vivo
Bulk 4T1.2 neo1-StfA1 cells were single cell cloned and quantitative RT-PCR was used to detect Stefin A1expression. High expressers were pooled (clones 1, 4, 7, 11, 12) and used for *in vivo* experiments along with the 4T1.2neo1-base vector (BV) bulk cell population as a control.

When Stefin A1 and BV clones were injected into the mammary glands of Balb/c mice there was no significant difference in primary tumor growth (Figure 24A,B), and even though Stefin A1 was induced in the 4T1.2-BV primary tumors (as expected), the enhanced expression was maintained in 4T1.2-StfA1 tumors (Figure 24C). Interestingly, both plasma calcium levels (Figure 25A) and lung and bone

metastases (Figure 25B,C) decreased in the over-expression lines. This indicated that over-expression of Stefin A1 decreases metastasis, in fact it almost totally inhibits bone metastasis with most spines having no detection of any tumor burden (by QPCR of the neomycin tag) and the return of plasma calcium concentrations to that of "normal" mice that do not have tumor burden. There are a number of hypotheses as to why increased Stefin A1 may decrease metastasis. Firstly, it was seen from task 2 that Stefin A1 is only seen in specific cell populations within a primary tumor. Expression in all cells prior to injection may inhibit cathepsins that are important in metastasis (eg cathepsin B, D, K). Alternatively, the cellular localization of stefin A1 may be altered, again resulting in the inhibition of cathepsins that are pro-metastatic. In base vector cells, the localised expression of Stefin A1 may be serving to inhibit the lysosomal activity of pro-apoptotic cathepsins (eg cathepsin L) and those involved in immune recognition/antigen presentation (eg cathepsin S). Another hypothesis is that Stefin A1 induction in 4T1.2 cells *in vivo* may just be a marker of an increased cathepsin activity. We are currently investigating cathepsin expression and activity in the mouse model to determine whether Stefin A co-localises with cathepsins in vivo and the specific cathepsins that have a role in metastasis.

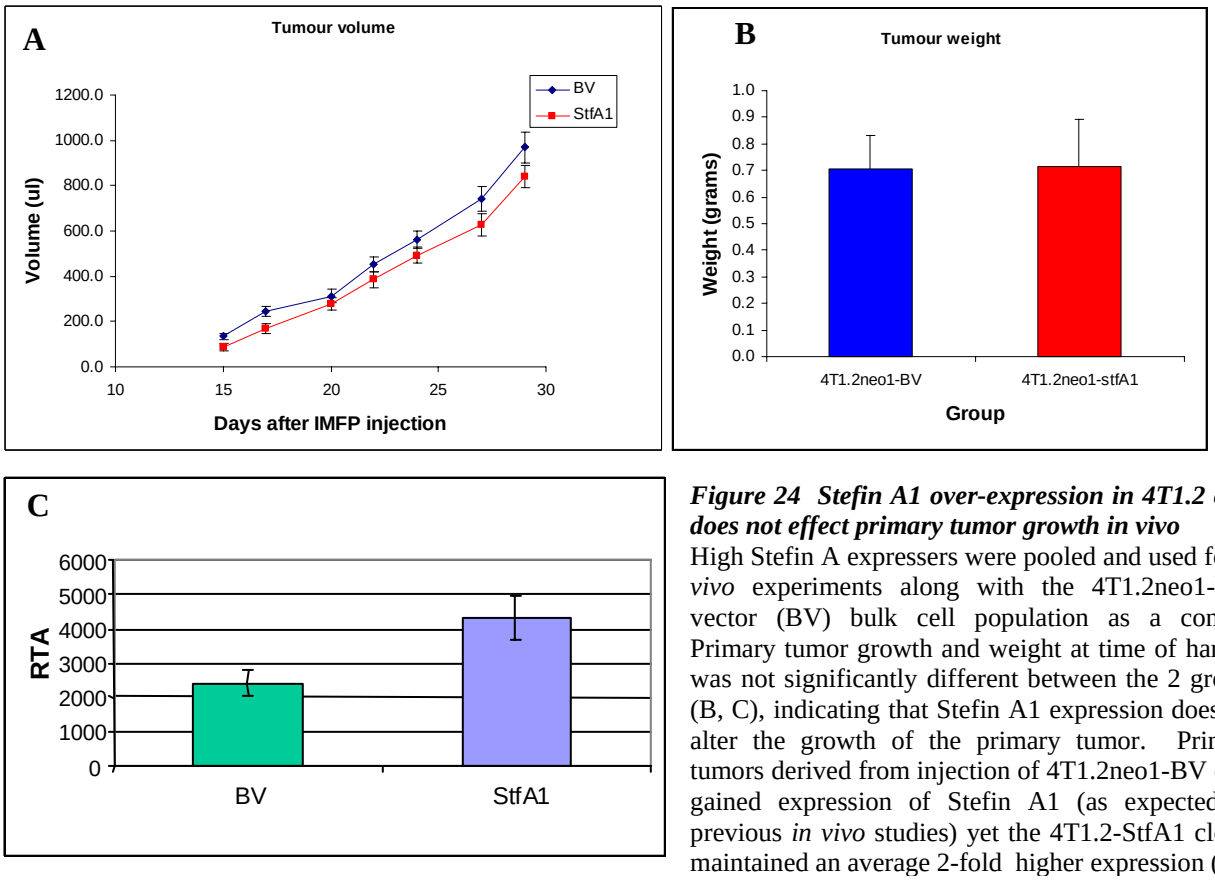

Figure 24 Stefin A1 over-expression in 4T1.2 cells does not effect primary tumor growth in vivo
High Stefin A expressers were pooled and used for *in vivo* experiments along with the 4T1.2neo1-base vector (BV) bulk cell population as a control. Primary tumor growth and weight at time of harvest was not significantly different between the 2 groups (B, C), indicating that Stefin A1 expression does not alter the growth of the primary tumor. Primary tumors derived from injection of 4T1.2neo1-BV cells gained expression of Stefin A1 (as expected by previous *in vivo* studies) yet the 4T1.2-StfA1 clones maintained an average 2-fold higher expression (C)

Due to the role of Stefin A as a cathepsin inhibitor it is important to determine if the enhanced expression in metastatic nodules is in response to increased cysteine cathepsin activity. We propose that Stefin A is acting as a protease sensing system and hence, a marker of the contribution of cathepsins to metastasis.
We quantitated the expression of cathepsins B, L, K and S in 67NR, 66cl4 and 4T1.2 primary tumours and found that transcript levels did not correlate with metastatic potential of the primary tumours (Figure 26A). However, when fluorogenic substrates were used to assay cathepsin activity in the same tissues, a significant increase in cathepsin B activity was found in the highly metastatic primary tumours compared to non-metastatic 67NR tumours (p=0.008) (Figure 26B). Conversely, cathepsin L activity decreased with increasing metastatic potential (p= 0.006) (Figure 26C) whilst cathepsin S activity was unchanged

(Figure 26D). Immunohistochemical analysis in 4T1.2 primary tumours revealed strong cathepsin B protein expression at the invasive front, but no expression was detected in areas not adjacent to surrounding stroma (Figure 27). Cathepsin B was expressed in matched spine metastases, with greatest intensity in tumour cells adjacent to bone and other stromal components (Figure 27). This pattern of expression was similar to that seen with Stefin A, where expression is greatest in tumour cells interacting with host stroma (Figure 27). To establish a functional connection between cathepsin B and Stefin A in primary and metastatic human tumours, we compared their expression by IHC and found co-localisation of Stefin A with cathepsin B in multiple invasive primary tumours (Figure 28A). This is consistent with Stefin A acting as a biomarker of elevated cathepsin B expression. Additionally, in lung metastases, where Stefin A is commonly expressed in tumour deposits interacting with stroma, cathepsin B was specifically expressed in the same deposits, as identified using serial sections (Figure 28B). In regions that were not interacting directly with the ECM or stroma, neither Stefin A nor cathepsin B expression was detectable (Figure 28C). Additionally, in lung metastases, where Stefin A is commonly expressed in tumor deposits interacting with stroma, cathepsin B was specifically expressed in the same deposits, as identified using serial sections (Figure 29A). In regions that were not interacting directly with the ECM or stroma, neither Stefin A nor cathepsin B expression was detectable (Figure 29B). This co-localisation was also observed in metastatic nodules in the murine model (data not shown).

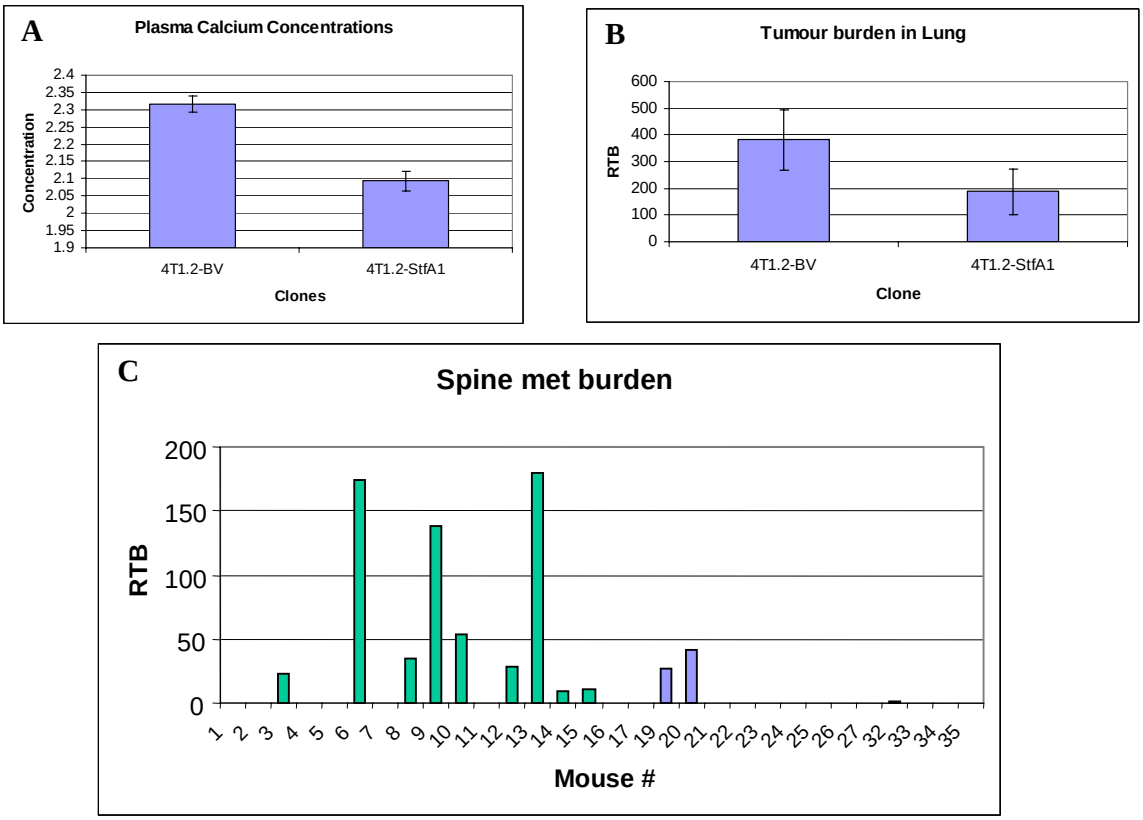

Figure 25 Stefin A1 over-expression in vitro leads to reduced lung and bone metastasis in vivo

A) The concentration of plasma calcium in all 30 mice was measured as an indication of distant metastatic involvement. As can be seen, mice injected with 4T1.2-StfA1 clones had reduced plasma calcium, in fact the concentration was equivalent to levels seen in mice that do not have tumor burden (~2.1). This indicates a decrease in metastatic burden and this was confirmed by realtime QPCR detection. In the lungs (B) there was a marked decrease in tumor burden (neomycin tagged tumor cells compared to vimentin signal). This effect was even greater in spine metastases, with an almost complete inhibition of spine metastases in the 4T1.2 cells over-expressing StfA1 (mice 16-35, blue)(C).

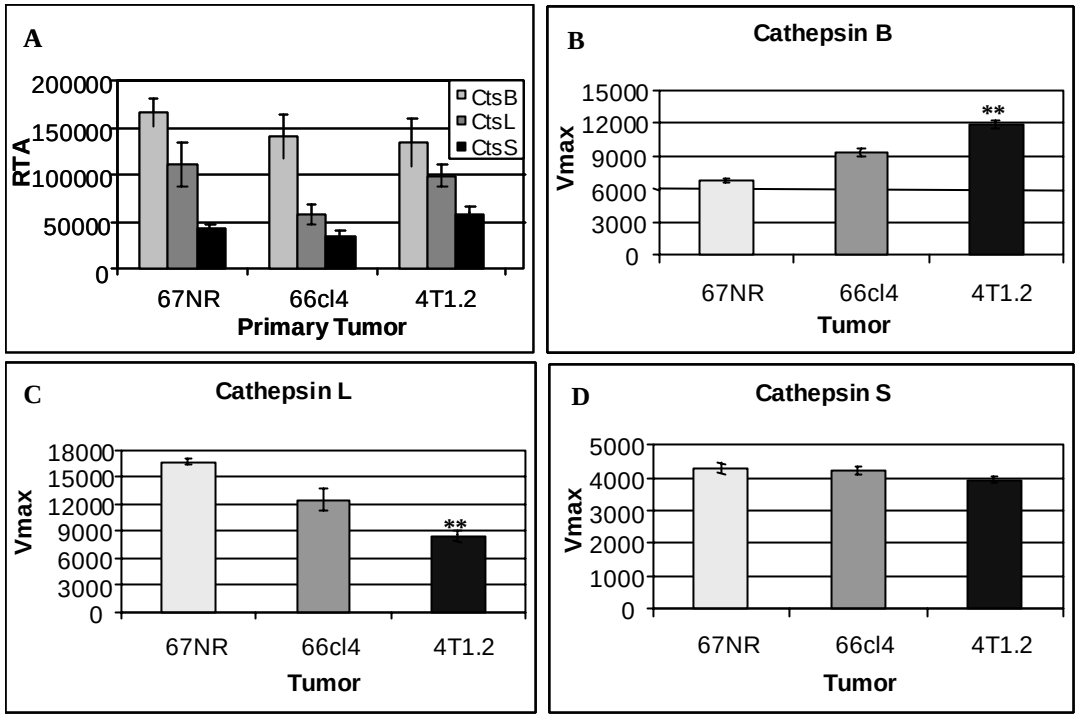

Figure 26 Cathepsin expression and activity in primary tumors
Snap frozen tissues (67NR, 66cl4, 4T1.2 primary tumors) were pulverized to a powder form in liquid nitrogen. To quantitate cathepsin transcripts, RNA was extracted and real time RT-PCR was used to determine cathepsin B (CtsB), L (CtsL) and S (CtsS) expression compared to GAPDH (A). For cathepsin activity assays, cells were lysed in the appropriate buffer (BioVision) and protein concentrations determined by Bradford assay. Lysates containing 50 mg protein were added to cathepsin B, L, and S activity assays utilizing fluorogenic substrates for detection of activity (BioVision) (B-D). ** Indicates P values of <0.01 between 67NR and 4T1.2 primary tumors.

Our future efforts will include determination of whether key cathepsin proteases and causing the induction of Stefin A and if inhibiting such proteases has therapeutic potential for treatment of metastatic breast cancer.

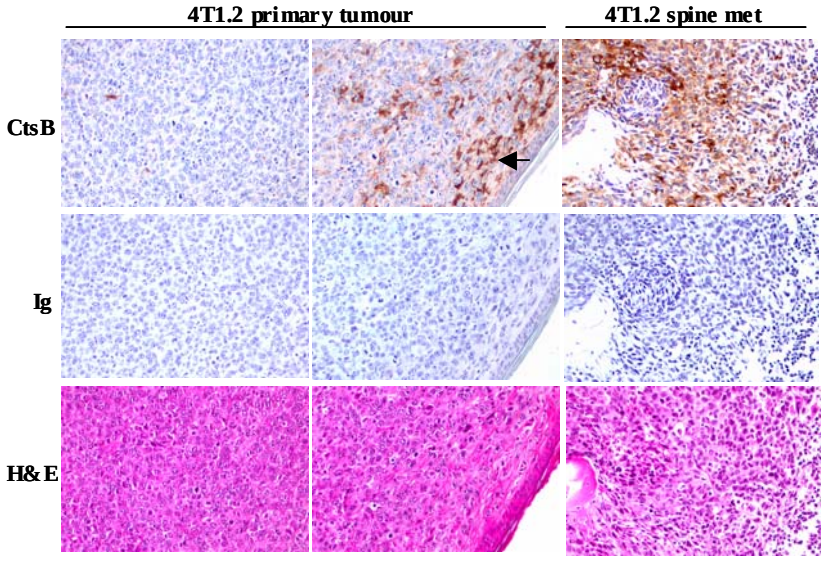

Figure 27 Cathepsin B expression in 4T1.2 primary tumours and spine metastases. Paraffin embedded primary and spine tissues were stained with rabbit anti-mouse cathepsin B (CtsB) or rabbit Ig isotype control. Two panels designated primary tumour represent two regions of the same tumour, either in the centre (left panel) or at the invasive front (indicated by the arrow) (centre panel).

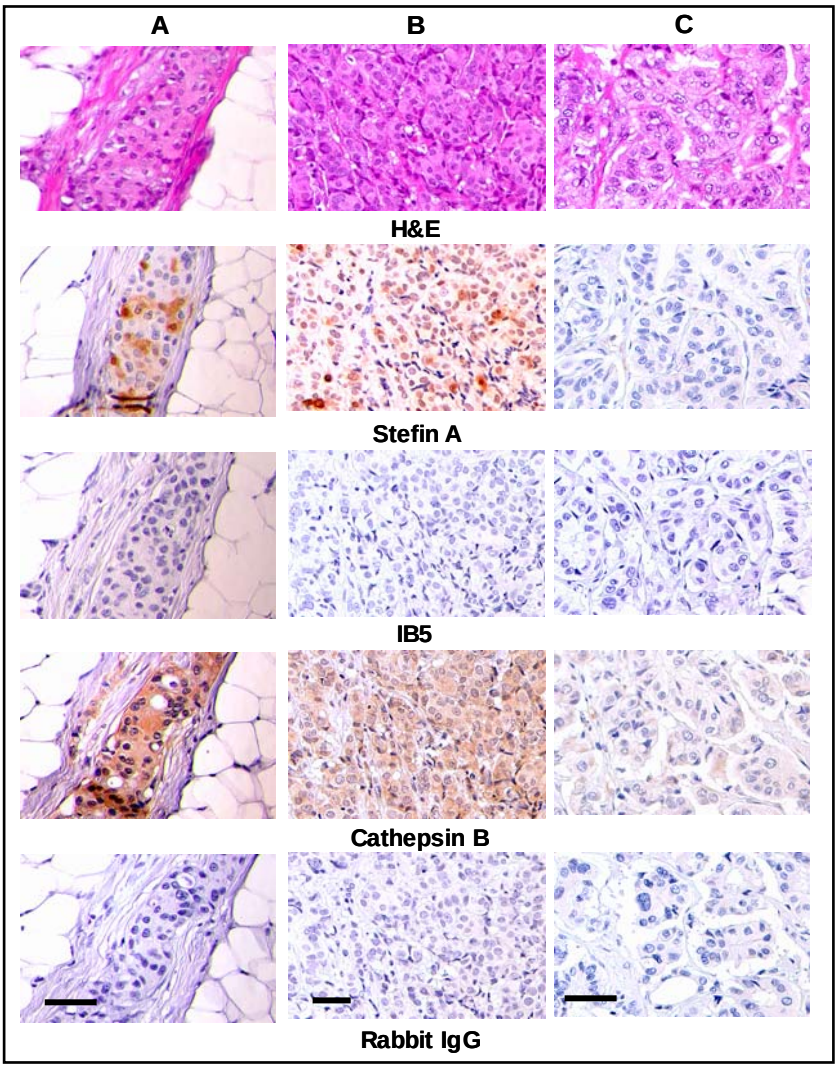

Figure 28 Cathepsin B expression in human primary tumors
Sections of formalin fixed, paraffin embedded primary breast tumors (A-C) were stained with Stefin A monoclonal antibody and 1B5 hybridoma supernatant as isotype control, or polyclonal anti-cathepsin B and rabbit IgG as a negative control. Signal was visualised with DAB and all tissues were counterstained with hematoxylin. Sample D exhibits no Stefin A protein and very little cathepsin B. Scale bar represents 50 μm.

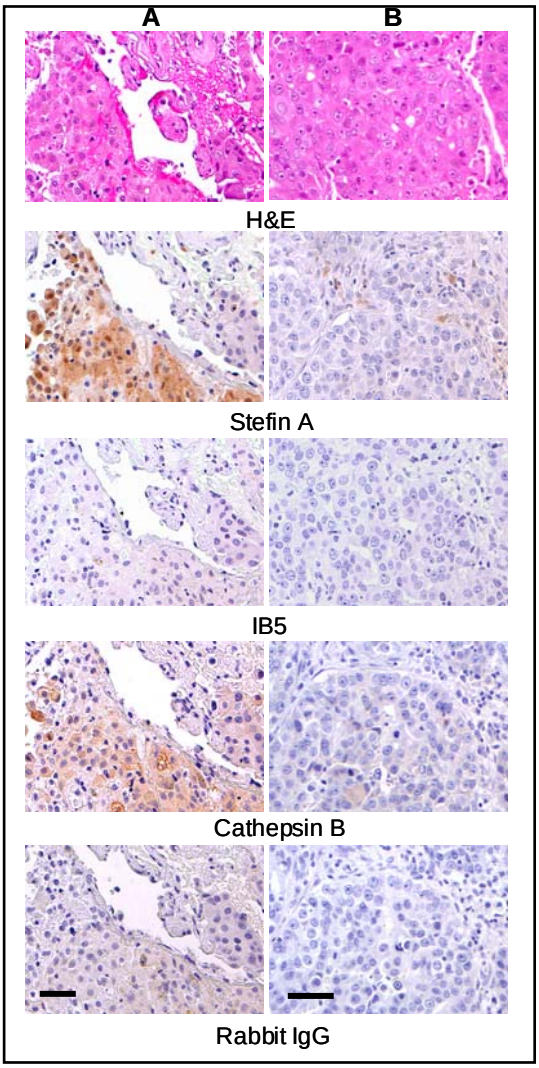

Figure 29 Cathepsin B co-localises with Stefin A in human lung metastases
Correlation of Stefin A and cathepsin B expression in paraffin embedded lung metastases using immunohistochemistry. Tumor deposits in contact with lung stroma express Stefin A (A) whereas the centre of the tumor is negative (B). Scale bar represents 50 μm.

ESTs (Potential Metastasis Suppressors)

The ability of Lrch2 and EST over-expression tumour cell lines to form primary tumours and to develop distant metastases was determined by an *in vivo* mouse study. Bulk cell populations were single cell cloned, expression was confirmed and clones pooled for *in vivo* work. When Lrch2 Flag Fwd (N-terminal), 4T1.2 EST Flag Rev (C-terminal) and BV clones were injected into the mammary glands of Balb/c mice there was no significant difference in primary tumor growth over 28 days (Figure 30A,B). This data confirms our hypothesis that the expression of neither EST nor Lrch2 has an effect on primary tumour growth and is consistent with the *in vitro* proliferation assay. At day 28, mice were culled and tissues (including lungs, spines and femurs) were harvested and snap frozen in liquid nitrogen subsequent to DNA extraction and real time QPCR amplification of the neomycin gene to detect tumor cell burden

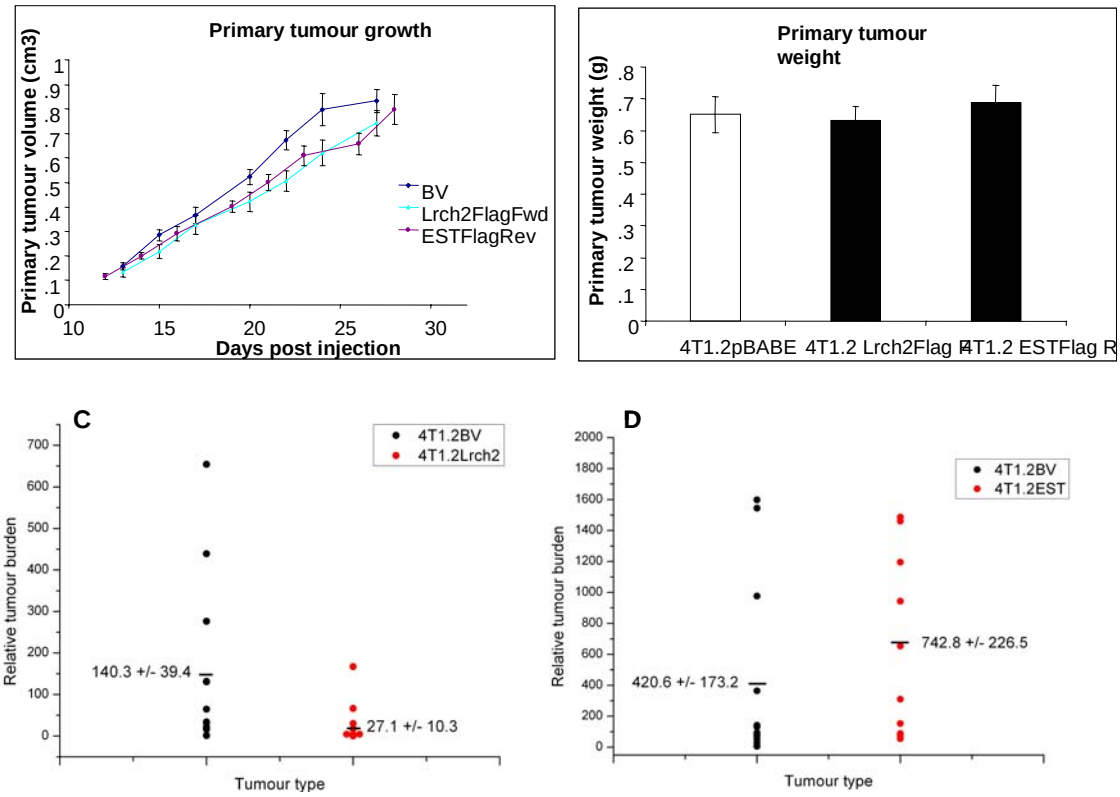

Figure 30. In vivo study. Balb/c mice (15 mice per group) were injected with 4T1.2 pBABE, 4T1.2 Lrch2 Flag Fwd or 4T1.2 EST Flag Rev cells to determine the ability of these cells to form metastases. **A.** Tumour growth was monitored by calliper measurements. Mice were culled and tissues were harvested for assay of metastatic burden on day 28. **B.** Average weights of the primary tumours at the end of the study indicate no difference between the three groups. **C.** QRT-PCR analysis of tumour burden in lung from mice bearing the modified cells 4T1.2 Lrch2 Flag Fwd (red dots) or the 4T1.2pBABE cells (black dots). **D.** QRT-PCR analysis of tumour burden in lung from mice bearing the modified cells 4T1.2 EST Flag Rev (red dots) or the 4T1.2pBABE cells (black dots). Average tumour burden +/- SE for all mice is shown in these figures

(4T1.2 cells are tagged with the neomycin resistance gene). Metastatic tumour burden was reduced significantly in the lungs of mice bearing 4T1.2 Lrch2 Flag Fwd tumours ($P<0.05$; Figure 30C) compared to the lungs of the 4T1.2pBABE mice. No statistical difference was seen in metastatic tumour burden for the mice with 4T1.2 EST Flag Rev tumours (Figure 30D). This indicated that over-expression of LRCH2 significantly decreases lung metastasis. This was also observed using histology, where representative primary tumors and lungs from 2 mice of each group of mice were paraffin embedded, sectioned and stained with hematoxylin and eosin. Representative sections of the lungs and primary tumour provide further evidence of the difference in metastatic ability of the modified cell lines (Figure 31). No morphological differences were seen in the primary tumours of the two mouse groups. The lungs for the base vector tumour bearing mice showed large metastatic lesions, however, few cells were found in the lungs of mice injected with 4T1.2 Lrch2 Flag Fwd, and these were close to the vasculature (Figure 31 lung metastases (1)), but they did not form large metastatic lesions. Combined these data reveal a marked difference in metastatic ability for the Lrch2 expressing cells to metastasize to the lung. RTQ-PCR and histology need to be completed for the other tissues (femurs and spine) to reveal more data on the suppressive role of Lrch2 in breast cancer metastasis.

In contrast, no differences were observed in metastatic tumour cells in the H&E stained lung sections from mice with 4T1.2 EST Flag Rev tumours compared to 4T1.2pBABE control cells (Figure 31). This reveals,

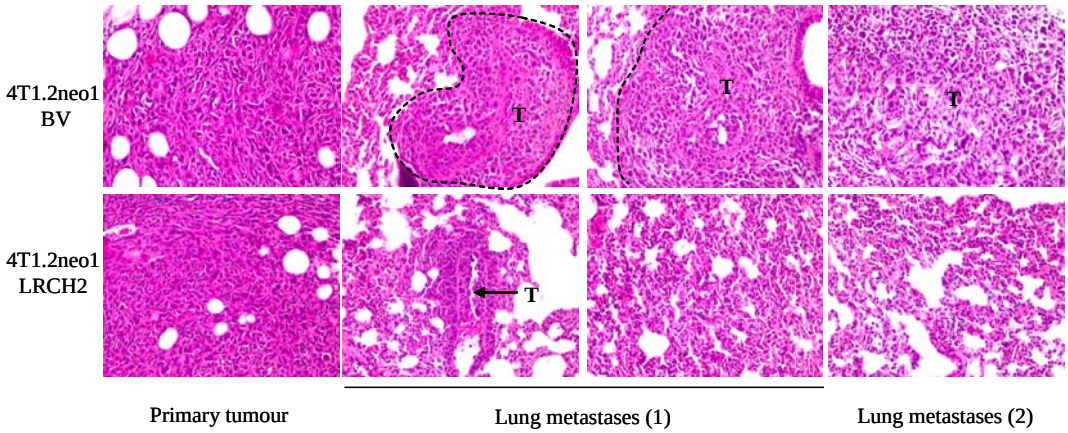

Figure 31. H&E staining of primary tumour and lungs for 4T1.2pBABE and 4T1.2 Lrch2 Flag Fwd. Primary tumour and lungs of two mice for each group were harvested and fixed in 10% buffered formalin overnight at 4°C, embedded in paraffin, sectioned and stained with hematoxylin and eosin to visualize cellular morphology. Lung metastases are indicated (T) and the dotted line marks tumour boundaries in the lung sections.

as we also showed with RTQ-PCR, that the EST did not have a suppressive role in the development of breast cancer metastases.
We will be further investigating Lrch2 as a potential metastasis suppressor. We now need to confirm the expression of this gene in human breast cancer, and the suppression in distant metastases, to determine the clinical validity of future investigations into the function of this gene in metastasis.

Using this Postdoctoral Fellowship, a number of genes have been identified that have roles in breast cancer metastasis. This work has already resulted in the granting of a Concept Award and will also form the basis of a number of Project Grants in the future.

KEY RESEARCH ACCOMPLISHMENTS

The key accomplishments during the course of this Postdoctoral Fellowship are as follows-

- Purification of epithelial, endothelial and "stromal" cells from primary tumors and lung and bone metastases derived from an *in vivo* model of breast cancer metastasis

- Microarray gene expression profiling of cell specific (tumor and endothelial cell) alterations with increasing metastatic propensity of primary tumors

- Identification of gene alterations that are associated with tumor growth in bone using Affymetrix microarray profiling. Analysis revealed significant suppression of defence/immune response genes that suggests evading immune recognition is required for successful metastasis to bone

- Realtime RT-PCR and/or *in situ* hybridisation verification of genes altered in primary tumor endothelium (FoxP1, LKB-1, MIF, SNAIL, PRL-3, LATS2) and epithelium (Stefin A1, BMP-4, DACH1, LNα5 and 2 ESTs)

- Realtime RT-PCR verification of genes suppressed in bone metastases (IRF7, interleukin receptors IL13rα1 and IL4rα, and chemokine ligands CCL7 and CXCL16) and verification of suppression of IRF7 protein in spine metastases by immunohistochemstry

- Verification that expression of the cathepsin inhibitor Stefin A (including the 3 murine homologs A1, A2 and A3) is induced in primary tumours that are metastatic to lung and bone, and is expressed at greater levels in matched metastases in a murine model of breast cancer metastasis.

- In human cancer, Stefin A expression is also enhanced throughout metastasis, with highest expression observed in metastases in lung and bone. Staining of a small cohort of primary breast cancers indicates that Stefin A expression predicts poor outcome and reduced disease-free survival ($p=<0.02$). Analysis of a large cohort is underway, and preliminary analysis of this independent set of samples also indicates that patients with primary tumors positive for Stefin A have an increased risk of recurrence ($P=<0.01$).

- Over-expression of Stefin A in tumor cells leads to a reduction in metastasis to lung and bone *in vivo*. This allows the hypothesis to be formed that Stefin A is a marker of the increased activity of cysteine proteases and that tipping the balance of protease:inhibitor interferes with metastatic progression. The interplay between cathepsins and their inhibitors may be important in breast cancer metastasis.

- Cathepsin B activity increases in highly metastatic primary tumors and Cathepsin B co-localises with Stefin A in primary tumors and lung and bone metastases in both the murine model and in human tissues.

- Over-expression of the novel gene Lrch2 suppresses lung metastasis *in vivo*

REPORTABLE OUTCOMES

Awards

2006 Travel Award of the 11th International Congress of Metastasis Research Society (MRS)

2005 Awarded US Army Department of Defense (DOD) Breast Cancer Research Program (BCRP) Concept Award

2005 Finalist- Cure Cancer Australia Young Researcher of the Year

2003 AACR Special Conference Scholar-in-Training Award (provided by the Avon Foundation).

Publications

Chia, J., Anderson, R., Kusuma, N., **Parker, B**., Bidwell, B., Zamurs, L., Nice, E., Pouliot, N. Evidence for a role of laminin-10 in the metastatic progression of breast tumors. *Am. J. Pathol.*, Submitted.

Parker, B.S., Bidwell, B.N., Slavin, J., Pouliot, N., Henderson, M., and Anderson, R.L. Enhanced expression of the cathepsin inhibitor Stefin A is associated with metastatic progression in breast cancer. *Clinical Cancer Research*, submitted.

Wu, X., Chen, H., **Parker, B.S**., Rubin, E., Zhu, T., Lee, J.S., Argani, P. and Sukumar, S. (2006). HOXB7, a homeodomain protein, is overexpressed in breast cancer and confers epithelial mesenchymal transition. *Cancer Research*, accepted with minor revision.

Eckhardt, B.L., **Parker, B.S**., van Laar, R.K., Restall, C.M., Natoli, A.L., Tavaria, M.D., Stanley, K.L., Sloan, E.K., Moseley, J.M., and Robin L. Anderson. (2005). Genomic analysis of a spontaneous model of breast cancer metastasis to bone reveals a role for the extracellular matrix. *Molecular Cancer Research*, 3, 1-13.

Parker BS, Argani P, Cook BP, Liangfeng H, Chartrand SD, Zhang M, Saha S, Bardelli A, Jiang Y, St Martin TB, Nacht M, Teicher BA, Klinger KW, Sukumar S and Madden SL (2004). Alterations in vascular gene expression in invasive breast carcinoma. *Cancer Research*, 64, 7857-7866.

Parker, B.S., Eckhardt, B.L. and Anderson, R.L. (2004). Models of breast cancer metastasis to bone: characterization of a clinically relevant model. In Bone Metastasis, Eds. G. Singh and F.W. Orr, Kluwer Press, The Netherlands.

Conference Presentations

Enhanced expression of the cathepsin inhibitor Stefin A is associated with metastasis in breast cancer. Parker, B.S, Bidwell, B.N, Slavin, J.L, Pouliot, N., Henderson, M. and Anderson, R.L. 11th International Congress of Metastasis Research Society, September 2006. Tokishima, Japan. Platform presentation.

Interplay between cathepsins and their inhibitor Stefin A regulates breast cancer metastasis to lung and bone. Parker, B.S., Bidwell, B.N., Pouliot, N.and Anderson, R.L. 18th Lorne Cancer Conference, February 2006. Lorne, Victoria, Australia.

Genetic alterations in tumor epithelium and host endothelium associated with metastatic progression in a murine model of breast cancer metastasis. Parker, B.S and Anderson, R.L. 4th Era of Hope Meeting for the Department of Defense (DOD) Breast Cancer Research Program (BCRP), June 2005. Philadelphia, Pennsylvania. Poster and platform presentation.

Cell specific gene expression profiling in a murine model of breast cancer metastasis. Parker, B.S. and Anderson, R.L. 10th International Congress of the Metastasis Research Society, September 2004. Genoa, Italy.

Aberrant gene expression in breast cancer endothelium. Parker, B.S., Madden, S.L., Sukumar, S.S. and Anderson, R.L. Advances in Breast Cancer Research: Genetics, Biology, and Clinical Implications (AACR Special Conference), 2003. Huntington Beach, CA, USA.

Aberrant gene expression in breast cancer endothelium . Parker, B.S., Madden, S.L., Sukumar, S.S. and Anderson, R.L. 5th Peter MacCallum Cancer Centre Symposium, November, 2003. Melbourne, Australia.

CONCLUSIONS

Considerable effort is aimed towards a determination of the molecular pathways that contribute to breast cancer metastasis. The lack of clinically relevant models of spontaneous metastasis to bone hinder these studies. In this study, we have used a validated murine model of spontaneous metastasis to identify gene candidates that contribute to metastatic progression. This study has investigated cell specific gene expression alterations during metastatic progression of breast cancer. Endothelial and epithelial cells have been successfully purified from primary breast tumors and lung and bone metastases and expression profiled using cDNA and Affymetrix microarrays.

A number of candidates have been identified as over-expressed or suppressed in tumor endothelium and in the tumor cells themselves during metastatic progression. Some of these have been verified by quantitative RT-PCR, *in situ* hybridisation and immunohistochemistry and are being analysed further for their functional role in metastasis, and for their role in human breast cancer. Particular interest for future studies are 3 groups of genes- the cathepsin proteases and their inhibitor Stefin A, interleukin receptors IL13rα1 and IL4rα and the interferon regulatory factor IRF7 and a novel gene that may have promise as a metastasis suppressor, Lrch2.

We have identified that the cysteine cathepsin inhibitor Stefin A is enhanced throughout metastatic progression. Our studies have confirmed that Stefin A is induced in metastatic primary tumors and is further enhanced in matched metastases to lung and bone, in both murine and human tumors. In fact, lack of Stefin A expression decreased risk of recurrence and improved patient outcome in a small cohort study. Co-localisation studies have shown that Stefin A co-localizes with cathepsin B in primary tumors and metastases in lung and bone and we have also detected enhanced activity of cathepsin B in highly metastatic tumors in our murine model. Our data implicate the cysteine cathepsins and their endogenous inhibitor Stefin A in breast cancer progression and form the basis of future studies into the prognostic value of Stefin A and the inhibition of cathepsins as a target for therapy of metastatic breast cancer.

The suppression of the group of genes involved in immune defence (IRF7 etc) in bone metastases when compared to expression at the primary site offers an interesting concept of successful formation of macrometastases. It is possible that in order to survive long enough for stimulating a growth environment in distant tissues, the tumor cells need to evade immune recognition. Therefore, our hypothesis is that retaining expression of these genes may lead to a suppression of metastasis *in vivo* and our future work will involve determination of how important this process is.

This work has many implications to breast cancer research. The use of a clinically relevant model of breast cancer metastasis was not only useful for finding gene candidates but is also of enormous importance in determining the functional role of such genes in the metastasis process. This has not been possible in other studies, and may be responsible for the lack of molecular markers as prognostic indicators and targets for treatment. This study has combined the use of a syngeneic model of spontaneous breast cancer metastasis with immunopurification of tumor and stromal cell populations. This allows for interactions of tumor cells with compatible stroma and the use of an immunocompetent model, two factors that have been found to be extremely important in cancer progression. Genes that have previously been associated with human cancer progression have been identified in this study and the fact that we have verified expression of one of our candidates in human breast cancer, with potential prognostic significance, reveals the clinical relevance of this model in investigating breast cancer metastasis.

REFERENCES

1. Kenny, P. A. and Bissell, M. J. Tumor reversion: correction of malignant behavior by microenvironmental cues. Int J Cancer, *107:* 688-695, 2003.
2. Schedin, P. and Elias, A. Multistep tumorigenesis and the microenvironment. Breast Cancer Res, *6:* 93-101, 2004.
3. Kim, J. B., Stein, R., and O'Hare M, J. Tumour-Stromal Interactions in Breast Cancer: The Role of Stroma in Tumourigenesis. Tumour Biol, *26:* 173-185, 2005.
4. Barcellos-Hoff, M. H. and Medina, D. New highlights on stroma-epithelial interactions in breast cancer. Breast Cancer Res, *7:* 33-36, 2005.
5. Alcaraz, J., Nelson, C. M., and Bissell, M. J. Biomechanical approaches for studying integration of tissue structure and function in mammary epithelia. J Mammary Gland Biol Neoplasia, *9:* 361-374, 2004.
6. Cukierman, E. A visual-quantitative analysis of fibroblastic stromagenesis in breast cancer progression. J Mammary Gland Biol Neoplasia, *9:* 311-324, 2004.
7. Kuperwasser, C., Chavarria, T., Wu, M., Magrane, G., Gray, J. W., Carey, L., et al. Reconstruction of functionally normal and malignant human breast tissues in mice. Proc Natl Acad Sci U S A, *101:* 4966-4971, 2004.
8. Orimo, A., Gupta, P. B., Sgroi, D. C., Arenzana-Seisdedos, F., Delaunay, T., Naeem, R., et al. Stromal fibroblasts present in invasive human breast carcinomas promote tumor growth and angiogenesis through elevated SDF-1/CXCL12 secretion. Cell, *121:* 335-348, 2005.
9. Yu, J. L. and Rak, J. W. Host microenvironment in breast cancer development: inflammatory and immune cells in tumour angiogenesis and arteriogenesis. Breast Cancer Res, *5:* 83-88, 2003.
10. Sinha, P., Clements, V. K., Miller, S., and Ostrand-Rosenberg, S. Tumor immunity: a balancing act between T cell activation, macrophage activation and tumor-induced immune suppression. Cancer Immunol Immunother, *54:* 1137-1142, 2005.
11. Lelekakis, M., Moseley, J. M., Martin, T. J., Hards, D., Williams, E., Ho, P., et al. A novel orthotopic model of breast cancer metastasis to bone. Clin Exp Metastasis, *17:* 163-170, 1999.
12. Eckhardt, B. L., Parker, B. S., van Laar, R. K., Restall, C. M., Natoli, A. L., Tavaria, M. D., et al. Genomic analysis of a spontaneous model of breast cancer metastasis to bone reveals a role for the extracellular matrix. Mol Cancer Res, *3:* 1-13, 2005.
13. Parker, B. S., Argani, P., Cook, B. P., Liangfeng, H., Chartrand, S. D., Zhang, M., et al. Alterations in vascular gene expression in invasive breast carcinoma. Cancer Res, *64:* 7857-7866, 2004.
14. Kargul, G. J., Dudekula, D. B., Qian, Y., Lim, M. K., Jaradat, S. A., Tanaka, T. S., et al. Verification and initial annotation of the NIA mouse 15K cDNA clone set. Nat Genet, *28:* 17-18, 2001.
15. Yang, Y. H., Dudoit, S., Luu, P., Lin, D. M., Peng, V., Ngai, J., et al. Normalization for cDNA microarray data: a robust composite method addressing single and multiple slide systematic variation. Nucleic Acids Res, *30:* e15, 2002.
16. Meehan, W. J. and Welch, D. R. Breast cancer metastasis suppressor 1: update. Clin Exp Metastasis, *20:* 45-50, 2003.
17. Samant, R. S., Debies, M. T., Hurst, D. R., Moore, B. P., Shevde, L. A., and Welch, D. R. Suppression of murine mammary carcinoma metastasis by the murine ortholog of breast cancer metastasis suppressor 1 (Brms1). Cancer Lett, 2005.
18. Shi, Y. and Massague, J. Mechanisms of TGF-beta signaling from cell membrane to the nucleus. Cell, *113:* 685-700, 2003.
19. Wu, K., Yang, Y., Wang, C., Davoli, M. A., D'Amico, M., Li, A., et al. DACH1 inhibits transforming growth factor-beta signaling through binding Smad4. J Biol Chem, *278:* 51673-51684, 2003.

20. Horner, A., Shum, L., Ayres, J. A., Nonaka, K., and Nuckolls, G. H. Fibroblast growth factor signaling regulates Dach1 expression during skeletal development. Dev Dyn, *225:* 35-45, 2002.
21. Bardelli, A., Saha, S., Sager, J. A., Romans, K. E., Xin, B., Markowitz, S. D., et al. PRL-3 expression in metastatic cancers. Clin Cancer Res, *9:* 5607-5615, 2003.

APPENDICES

Belinda S. Parker

5 Frost Crt, Bundoora, Victoria 3083
Ph: 0402849305 (m) 03) 96561285 (w)
Fax: 03) 96561411
DOB: 13/03/75
Belinda.parker@petermac.org

EDUCATION AND POSTDOCTORAL EXPERIENCE

Peter MacCallum Cancer Centre
Senior Postdoctoral Fellow **2003-present**
Department: Research (Breast Cancer Program)
Field of Study: Breast Cancer
PI: Dr. Robin Anderson

Johns Hopkins Univerisity, MD, USA
Postdoctoral Fellow **2001-2003**
Department: Oncology
Field of Study: Breast Cancer
PI: Prof. Sara Sukumar

La Trobe University
Doctorate of Philosophy in Biochemistry **1998-2001**
Department: Biochemistry
Project: "Molecular and Cellular Studies of DNA Damage Induced by Mitoxantrone"
Supervisors: Prof. D.R. Phillips and Dr. S.M. Cutts

La Trobe University
Bachelor of Science (Honours) **1998-2001**
Department: Biochemistry
Project: ""
Supervisor: Prof. Don Phillips
Awarded First-Class Honours (H1)

La Trobe Univerisity
Bachelor of Science (Biological) **1997**
Majors: Biochemistry, Human Genetics

AWARDS/FELLOWSHIPS

- Travel Award of the 11th International Congress of Metastasis Research Society (MRS) **2006**
- US Army Department of Defense (DOD) Breast Cancer Research Program (BCRP) Concept Award **2005**
- Finalist- Cure Cancer Australia Young Researcher of the Year **2005**
- AACR Special Conference Scholar-in-Training Award (provided by the Avon Foundation) **2003**
- Awarded - Department of Defense Breast Cancer Research Program (BCRP) Postdoctoral Fellowship (July 2003-July 2006) **2003**
  - Susan Komen Foundation Postdoctoral Fellowship (declined)
  - Peter Doherty Postdoctoral Fellowship (March 2003-July 2003 then declined)
- Australian Society of Biochemistry and Molecular Biology (ASBMB) Travel Fellowship **2000**
- La Trobe University Postgraduate Scholarship (1998-2001) **1998**

MEMBERSHIPS/COMMITTEES

- Metastasis Research Society (MRS) member
- Australian Society of Medical Research (ASMR) member
- Australian Society of Biochemistry and Molecular Biology (ASBMB) member
- Peter MacCallum Postdoctoral Committee
- Peter MacCallum Infrastructure Committee
- Peter MacCallum Microarray Committee
- Peter MacCallum Tumour Biology Student Committee

SCIENTIFIC PUBLICATIONS

Chia, J., Anderson, R., Kusuma, N., **Parker, B**., Bidwell, B., Zamurs, L., Nice, E., Pouliot, N. Evidence for a role of laminin-10 in the metastatic progression of breast tumors. *Am. J. Pathol.,* Submitted.

Parker, B.S., Bidwell, B.N., Slavin, J., Pouliot, N., Henderson, M., and Anderson, R.L. Enhanced expression of the cathepsin inhibitor Stefin A is associated with metastatic progression in breast cancer. *Clinical Cancer Research,* submitted.

Wu, X., Chen, H., **Parker, B.S**., Rubin, E., Zhu, T., Lee, J.S., Argani, P. and Sukumar, S. (2006). HOXB7, a homeodomain protein, is overexpressed in breast cancer and confers epithelial mesenchymal transition. *Cancer Research,* accepted with minor revision.

Eckhardt, B.L., **Parker, B.S**., van Laar, R.K., Restall, C.M., Natoli, A.L., Tavaria, M.D., Stanley, K.L., Sloan, E.K., Moseley, J.M., and Robin L. Anderson. (2005). Genomic analysis of a spontaneous model of breast cancer metastasis to bone reveals a role for the extracellular matrix. *Molecular Cancer Research*, 3, 1-13.

Parker BS, Argani P, Cook BP, Liangfeng H, Chartrand SD, Zhang M, Saha S, Bardelli A, Jiang Y, St Martin TB, Nacht M, Teicher BA, Klinger KW, Sukumar S and Madden SL (2004). Alterations in vascular gene expression in invasive breast carcinoma. *Cancer Research,* 64, 7857-7866.

Parker, B.S., Eckhardt, B.L. and Anderson, R.L. (2004). Models of breast cancer metastasis to bone: characterization of a clinically relevant model. In Bone Metastasis, Eds. G. Singh and F.W. Orr, Kluwer Press, The Netherlands.

Parker, B.S., Rephaeli, A., Nudelman, A., Phillips, D.R. and Cutts, S.M. (2004). Formation of mitoxantrone adducts in human tumor cells: Potentiation by AN-9 and DNA methylation. *Oncology Research*, 14, 279-290.

Parker, B.S., Buley, T., Evison, B.J., Cutts, S.M., Neumann, G.M., Iskander, M.N. and Phillips, D.R. (2004). A molecular understanding of mitoxantrone-DNA adduct formation: Effect of cytosine methylation and flanking sequences. *J. Biol. Chem.* 279, 18814-18823.

Waly, M., Olteanu, H., Banerjee, R., Choi, S.-W., Mason, J.B., **Parker, B.S**., Sukumar, S., Shim, S., Sharma, A., Benzecry, J.M., Power-Charnitsky, V.-A. and Deth, R.C. (2004). Activation of methionine synthase by insulin-like growth factor-1 and dopamine: A target for neurodevelopmental toxins and thimerosal. *Molecular Psychiatry*, 9, 358-370.

Parker, B.S., Cutts, S.M., Nudelman, A., Rephaeli, A., Phillips, D.R. and Sukumar, S. (2003). Mitoxantrone mediates Demethylation and re-expression of cyclin D2, estrogen receptor and 14-3-3σ in breast cancer cells. *Cancer Biol. & Ther.* 2(3), 259-263.

Parker, B.S. and Sukumar, S. (2003). Distant metastasis in breast cancer: Molecular mechanisms and a search for therapeutic targets. *Cancer Biol. & Ther.* 2(1), 14-21.

Parker, B.S., Cutts, S.M. and Phillips, D.R. (2001). Cytosine methylation enhances mitoxantrone-DNA adduct formation at CpG dinucleotides. *J. Biol. Chem.* 276(19), 15953-15960.

Cutts, S.M., Parker, B. S., Swift, L. P., Kimura, K. and Phillips, D.R. (2000). Structural requirements for the formation of anthracycline-DNA adducts. *Anticancer Drug Design*. 15(5), 373-386.

Parker, B.S., Cutts, S.M., Cullinane, C. and Phillips, D.R. (2000). Formaldehyde activation of mitoxantrone yields CpG and CpG specific DNA adducts. *Nucleic Acids Research* 28, 982-990.

Parker, B.S., Cullinane, C. and Phillips, D.R. (1999). Formation of DNA adducts by formaldehyde-activated mitoxantrone. *Nucleic Acids Research* 27, 2918-2923.

ONGOING RESEARCH SUPPORT

- DOD/BCRP- Postdoctoral Fellowship (DAMD17-03-1-0473)
  Title: Stromal gene expression in primary breast tumours that metastasize to bone
  July 2003-July 2006
  Role: PI
- DOD/BCRP- Concept Award (W81XWH-05-1-0444)
  Title: The role of Stefin A in breast cancer metastasis
  July 2005-July 2006
  Role: PI

CONFERENCE PRESENTATIONS

Interplay between cathepsins and their inhibitor Stefin A regulates breast cancer metastasis to lung and bone. Parker, B.S., Bidwell, B.N., Pouliot, N.and Anderson, R.L. 18th Lorne Cancer Conference, February 2006. Lorne, Victoria, Australia.

Genetic aleteration in tumor epithelium and host endothelium associated with metastatic progression in a murine model of breast cancer metastasis. Parker, B.S and Anderson, R.L. 4th Era of Hope Meeting for the Department of Defense (DOD) Breast Cancer Research Program (BCRP), June 2005. Philadelphia, Pennsylvania. Poster **and** platform presentation

Cell specific gene expression profiling in a murine model of breast cancer metastasis. Parker, B.S. and Anderson, R.L. 10th International Congress of the Metastasis Research Society, September 2004. Genoa, Italy.

Aberrant gene expression in breast cancer endothelium . Parker, B.S., Madden, S.L., Sukumar, S.S. and Anderson, R.L. 5th Peter MacCallum Cancer Centre Symposium, November, 2003. Melbourne, Australia.

Aberrant gene expression in breast cancer endothelium. Parker, B.S., Madden, S.L., Sukumar, S.S. and Anderson, R.L. Advances in Breast Cancer Research: Genetics, Biology, and Clinical Implications (AACR Special Conference), 2003. Huntington Beach, CA, USA.

Enhancement of drug-DNA binding at methylated cytosine residues by the CpG specific anticancer drug mitoxantrone. Parker, B. S., Cutts, S. M. and Phillips, D.R. Annual Conference of the American Association of Cancer Research, March 2001. New Orleans, LS, USA.

The role of CpG methylation on mitoxantrone-DNA adduct formation. Parker, B.S., Swift, L. P., Cutts, S. M. and Phillips, D.R. Australian Society of Biochemistry and Molecular Biology Annual Conference, December 2000. Wellington, New Zealand.

Formaldehyde mediated DNA alkylation by mitoxantrone. Parker, B.S., Cullinane, C. and Phillips, D.R. Molecular Determinants of Sensitivity to Antitumour Agents, American Association of Cancer Research, March, 1999. Whistler, Canada

Molecular and cellular studies of the activation of mitoxantrone by formaldehyde. Parker, B.S., Cullinane, C. and Phillips, D.R. 11th Lorne Cancer Conference, Feb, 1999. Lorne, Australia

REFEREES

Dr. Robin Anderson
Head, Cancer Biology
Department of Research
Peter MacCallum Cancer Center
St Andrews Place
East Melbourne, 3002
Phone: 61 (0)3 96561286
Email: robin.anderson@petermac.org

Prof. Sara Sukumar
Professor of Oncology
Sidney Kimmel Comprehensive
Cancer Center at Johns Hopkins
1650 Orleans St
Baltimore, MD, 21231, USA
Phone: 11 410 6142479
Email: sukumsa@jhmi.edu

Professor Don R. Phillips
Reader in Biochemistry
La Trobe University
Bundoora, 3086
Australia
Phone: 61-3-9479 2182
Email: D.Phillips@latrobe.edu.au

Dr. Suzanne M. Cutts
Research Associate
School of Biochemistry
La Trobe University
Bundoora, 3086
Australia
Phone: 61-3-9479 1182
Email: scutts@bioserve.latrobe.edu.au

Clone ID	Genbank ID	Common	Description	Fold Difference	P value
Proteolysis					
BG074171	DV064073	Stfa1	Stefin A1 (Stfa1) mRNA	7.61	0.007
BG071209		Lap3	leucine aminopeptidase 3	1.692	0.007
BG072453	BC061493	Ephx1	epoxide hydrolase 1, microsomal	0.545	0.001
BG065831	AK145843	Pep4	peptidase 4	0.466	0.005
BG087340		Adam10	a disintegrin and metalloprotease domain 10	0.595	0.005
C76810	AB021709	Adam17	a disintegrin and metalloproteinase domain 17	0.34	0.003
Development					
BG071729	BC053384	Mater	maternal effect gene	2.116	0.004
BG065000	BC058708	Abr	active BCR-related gene	0.546	0.001
BG078804		Bmp4	bone morphogenetic protein 4	0.406	0.000
BG065879	BC094319	Eomes	eomesodermin homolog (Xenopus laevis)	1.968	0.006
BG076673		Foxm1	forkhead box M1	0.646	0.000
Cytoskeletal organisation/cell polarity/adhesion					
BG066360	AK028831	Arhgap8	Rho GTPase activating protein 8	1.826	0.004
AW546524		ARHGEF3	Rho guanine nucleotide exchange factor 3	1.818	0.002
BG085804		Arpc4	actin related protein 2/3 complex, subunit 4	0.522	0.008
BG064070	AK004554	Actr3	ARP3 actin-related protein 3 homolog	0.311	0.006
BG083452	BC060713	Dlgh3	discs, large homolog 3	2.01	0.000
BG068578	AK145707	Vil2	villin 2	2.679	0.002
AW557174	AF464160	Pcdhgb1	protocadherin gamma subfamily B, 1	1.885	0.003
BG073255	AK053325	Tm4sf8	transmembrane 4 superfamily member 8	1.879	0.003
BG065503	AK136315	Itgb5	integrin beta 5	0.282	0.008
BG073671	BC037475	Mfge8	milk fat globule-EGF factor 8 protein	2.192	0.007
AW553617	AB035511	Lu	Lutheran blood group	1.768	0.001
BG077621	AK147150	Lmna	lamin A	0.373	0.006
BG082584	NM_025276	Evpl	envoplakin	2.456	0.007
AU042820	AK172052	Rap1gds1	RAP1, GTP-GDP dissociation stimulator 1	0.438	0.000
Nucleosome assembly/nucleotide biosynthesis					
BG072171	BC052833	Hdc	histidine decarboxylase	6.236	0.003
BG073886	AK161084	Hp1bp3	heterochromatin protein 1, binding protein 3	1.518	0.004
AW557161	AK085381	Ctps2	cytidine 5'-triphosphate synthase 2	0.527	0.002
BG076632	AK138911	Adcy7	adenylate cyclase 7	0.385	0.005
Cell cycle/replication/DNA repair					
BG066894	AK220441	Morf4l1	mortality factor 4 like 1	1.547	0.006
BG075820	BC059934	Dach1	dachshund 1 (Drosophila)	2.298	0.004
BG078524	AK038348	Ets2	E26 avian leukemia oncogene 2, 3' domain	0.471	0.000
BG077759	AK084092	Mapre1	microtubule-associated protein, RP/EB family, 1	2.106	0.007
BG077618	AK079306	Mel	cell line NK14 derived transforming oncogene	0.571	0.005
AW538347	BC026649	E2f4	E2F transcription factor 4	0.556	0.001
BG077512	AF100694	Ruvbl1	RuvB-like protein 1	0.406	0.006
BG067384	AK049992	Pnkp	polynucleotide kinase 3'- phosphatase	0.544	0.006
BG071892	AK145591	Rad21	RAD21 homolog (S. pombe)	1.661	0.008
BG084231	AK141176	Rbbp4	retinoblastoma binding protein 4	1.84	0.002
BG084537	X72711	Recc1	replication factor C 1	1.576	0.009
BG074668	BC055318	Mcm2	minichromosome maintenance deficient 2 mitotin	0.517	0.004
Transcription/translation					
BG085841	AK031731	Nfe2l2	nuclear, factor, erythroid derived 2, like 2	0.205	0.002
BG087147	DV039263	Polr2g	polymerase (RNA) II polypeptide G	1.907	0.004
BG085094	AK136400	Psmd10	proteasome 26S subunit, non-ATPase, 10	1.742	0.004
BG063185	AK036592	Tceb3	transcription elongation factor B (SIII), peptide 3	0.589	0.006
BG087186	AK079075	Nr1d2	nuclear receptor subfamily 1, group D, member 2	0.465	0.004

Clone ID	Genbank ID	Common	Description	Fold Difference	P value
BG085367	AK154023	Snrpe	small nuclear ribonucleoprotein E	2.107	0.002
BG088147	M32309	Zfx	zinc finger protein X-linked	0.349	0.004
BG085518	DV067285	Eraf	erythroid associated factor	3.764	0.004
BG064438	AK048512	Rod1	ROD1 regulator of differentiation 1	0.386	0.004
BG086478	AK032059	Gspt1	G1 to phase transition 1	0.599	0.007
BG081111	AK083930	Top1	topoisomerase (DNA) I	0.528	0.001
BG088029	BF121988	Rpl7	ribosomal protein L7	2.044	0.004
BG085364	CA481590	Rplp2	ribosomal protein, large P2	2.007	0.004
BG072985	AK135460	Rpl7	ribosomal protein L7	1.924	0.003
BG077028	AK164483	Rpl44	ribosomal protein L44	1.909	0.003
BG077771	AK019964	Rrbp1	ribosome binding protein 1	1.514	0.002
BG086142	CA786550	Rpl23	ribosomal protein L23	1.597	0.002
BG073626	AK138355	Rps6ka3	ribosomal protein S6 kinase polypeptide 3	0.252	0.003
BG084428	AK141200	Ddx52	DEAD (Asp-Glu-Ala-Asp) box polypeptide 52	1.888	0.007
BG082703	AK129220	Ddx46	DEAD (Asp-Glu-Ala-Asp) box polypeptide 46	0.475	0.007
BG064223	NM_019553	Ddx21	DEAD (Asp-Glu-Ala-Asp) box polypeptide 21	0.374	0.000
BG066159		Eif2s2	eukaryotic translation initiation factor 2, subunit 2 (beta)	1.604	0.001
BG086385	AF193344	Eif2ak4	eukaryotic translation initiation factor 2 alpha kinase 4	0.517	0.001
BG086674	NM_007907	Eef2	eukaryotic translation elongation factor 2	0.436	0.000
BG084597	AK134065	Mrps17	mitochondrial ribosomal protein S17	2.054	0.000
BG074295	AK172097	Mrpl49	mitochondrial ribosomal protein L49	1.577	0.009
BG080951	NM_146217	Aars	alanyl-tRNA synthetase	0.587	0.005
BG072592	BC085495	Rpl3	ribosomal protein L3	0.48	0.003
BG086177	BC098497	Rpl3	ribosomal protein L3	0.378	0.001
BG088006	AK147826	Statip1	signal transducer and activator of transcription int prot 1	1.882	0.010
Protein modification/transport/signalling					
BG070260	AK171630	Fbxo34	F-box only protein 34	0.576	0.010
BG064722	AK148306	Smt3h1	SMT3 (supressor of mif two, 3) homolog 1	4.115	0.001
BG064723	AK148306	Smt3h1	SMT3 (supressor of mif two, 3) homolog 1	3.517	0.000
BG077854	BC042601	Ate1	arginine-tRNA-protein transferase 1	1.699	0.009
BG080240	AK168690	Mdm2	transformed mouse 3T3 cell double minute 2	0.53	0.001
BG082615	CF584400	Dnajb9	DnaJ (Hsp40) homolog, subfamily B, member 9	0.387	0.003
BG077186	AK167910	Hsp8	heat shock protein 8	0.341	0.010
BG078043	XM_354671	Hectd1	HECT domain containing 1	1.741	0.003
BG065099	BC062887	Clk	CDC-like kinase	0.51	0.007
BG065427	AK045011	Acp6	acid phosphatase 6, lysophosphatidic	0.639	0.001
BG064043	AK153307	Limk1	LIM-domain containing, protein kinase	0.564	0.008
BG070547	NM_001025566	Chk	choline kinase	0.459	0.001
BG064270	AK148853	Mapk1	mitogen activated protein kinase 1	0.401	0.005
BG085457	NM_021462	Mknk2	MAP kinase-interacting serine/threonine kinase 2	0.402	0.003
BG079186	NM_010336	Edg2	endothelial diff, lysophos acid G-protein- receptor, 2	1.859	0.003
BG084165	Y18365	Cd97	CD97 antigen	0.598	0.009
BG072244	BC054805	Calm1	calmodulin 1	0.528	0.000
BG085452	AK088814	Tram1	translocating chain-associating membrane protein 1	0.515	0.001
BG064125	BC054104	Scamp4	secretory carrier membrane protein 4	0.48	0.009
BG074832	BC046417	Vps33a	vacuolar protein sorting 33A (yeast)	0.552	0.004
BG083295	AK165361	Ndufb5	NADH dehydrogenase 1 beta subcomplex, 5	2.099	0.002
BG087636	CA480457	Ndufb9	NADH dehydrogenase 1 beta subcomplex, 9	2.053	0.003
BG067327	AK158832	Arl6	ADP-ribosylation factor-like 6	0.652	0.004
BG065398	BC006675	Copb2	coatomer protein complex, subunit beta 2 (beta prime)	0.625	0.002
BG083225	AK147989	Vps26	vacuolar protein sorting 26 (yeast)	0.534	0.009
BG064129	AK154972	Gosr1	golgi SNAP receptor complex member 1	0.43	0.003

Clone ID	Genbank ID	Common	Description	Fold Difference	P value
BG080231	NM_008876	Pld2	phospholipase D2	0.571	0.002
BG068990		Supt6h	suppressor of Ty 6 homolog (S. cerevisiae)	0.322	0.000
BG064837	AK080936	Stip1	stress-induced phosphoprotein 1	1.64	0.003
BG066205	AK078499	Mrpl10	mitochondrial ribosomal protein L10	1.673	0.001
BG074631	AK145930	Slc4a2	solute carrier family 4 (anion exchanger), member 2	0.512	0.000
BG086960	AK135137	Atp6v1h	ATPase, H+ transporting, lysosomal 50/57kDa, V1 H	0.423	0.006
BG080311	M14757	Abcb1b	ATP-binding cassette, sub-family B (MDR/TAP), 1B	0.252	0.006
BG082389	CA786563	Atp5l	ATP synthase, mitochondrial F0 complex, subunit g	2.562	0.001
Cellular defense/apoptosis					
BG087429	BC043338	C3	complement component 3	3.56	0.004
BG085842		Ifnar1	interferon (alpha and beta) receptor 1	0.429	0.000
AW539333	BC013715	Oas1a	2'-5' oligoadenylate synthetase 1A	0.415	0.000
BG084405		Birc2	baculoviral IAP repeat-containing 2	1.532	0.006
BG088003	U35846	Api5	apoptosis inhibitor 5	0.523	0.003
BG063869	AK146992	Apg7l	autophagy 7-like (S. cerevisiae)	0.463	0.002
Metabolism					
BG063331	AK087454	Ahcyl1	S-adenosylhomocysteine hydrolase-like 1	0.653	0.004
BG087002	AK031670	Ndufv2	NADH dehydrogenase (ubiquinone) flavoprotein 2	2.098	0.007
BG073682	BC058360	Mat2a	methionine adenosyltransferase II, alpha	0.450	0.0002
BG077312	AK168720	Cox7c	cytochrome c oxidase, subunit VIIc	2.841	0.001
BG063843	AK009614	Cox7a2l	cytochrome c oxidase subunit VIIa polypeptide 2-like	2.235	0.0003
BG085742	AK076308	Thsd2	thrombospondin, type I, domain 2	1.684	0.009
BG075227	AK136193	Dld	dihydrolipoamide dehydrogenase	0.579	0.004
BG087256	AK049299	Abce1	ATP-binding cassette, sub-family E (OABP), member 1	0.463	0.0006
AW539350	AK152652	B4galt5	UDP-Gal:betaGlcNAc beta 1,4-galactosyltransferase, 5	0.451	0.001
BG063961		Man1a	mannosidase 1, alpha	0.368	0.003
Miscellaneous					
BG077363	AK087166	Brms1	breast cancer metastasis-suppressor 1	0.426	0.002
BG064726	BC026571	Snx17	sorting nexin 17	0.522	0.000
BG064642	AK163685	Pcyt1a	phosphate cytidylyltransferase 1, choline, alpha isoform	0.428	0.004
BG088166	AB093238	Lysal1	lysosomal apyrase-like 1	0.563	0.005
BG074344	AK146799	Msln	mesothelin	0.554	0.007
BG077623	AK146626	Hprt	hypoxanthine guanine phosphoribosyl transferase	0.518	0.005
BG087058	AK053908	Cryzl1	crystallin, zeta (quinone reductase)-like 1	0.509	0.001
BG085471	BC010331	Rnh1	ribonuclease/angiogenin inhibitor 1	0.494	0.001
BG076829	AF004927	Oprs1	opioid receptor, sigma 1	0.491	0.006
BG080793	AK035516	Csnk1e	casein kinase 1, epsilon	0.463	0.003
BG067953	AK168470	Tex292	testis expressed gene 292	0.38	0.001
BG081794	BC003247	Mclc	Mid-1-related chloride channel 1	0.37	0.007
BG065008	AK172662	Mkln1	muskelin 1, intracellular mediator containing kelch motifs	0.586	0.007
BG075350	AK171747	Gdi3	guanosine diphosphate (GDP) dissociation inhibitor 3	0.386	0.002
BG083544	AK145742	Snap23	synaptosomal-associated protein 23	0.574	0.008
BG074749	AK170193	Niban	niban protein	0.526	0.006
BG071061	AK141177	Ubp1	upstream binding protein 1	1.5	0.004

Table 1S- Genes altered in highly metastatic epithelial cells. Microarray profiling of transcript alterations in immunopurified epithelial cells from primary tumors that metastasize to lung and bone when compared to weakly or non-metastatic tumors. Fold difference indicates expression in highly metastatic tumors over expression in weakly or non-metastatic tumors.

Clone ID	Genbank ID	Common	Fold Difference	P value
BG071883	CA787144	RIKEN cDNA 1500015O10 gene	3.201	0.00598
BG088381	DV062528	RIKEN cDNA 2010100O12 gene	2.896	0.00287
BG069790	AK148847	RIKEN cDNA 2900070E19 gene	2.744	0.00103
BG078565	CA491491	RIKEN cDNA 1810004I06 gene	2.647	0.0044
BG066752	XM_144267	RIKEN cDNA 4933407H18 gene	2.549	0.00232
BG066777	AK172652	cDNA sequence BC027163	2.299	0.00509
BG070480	DV038944	RIKEN cDNA 1110001C03 gene	2.293	0.00587
BG064421	BQ174439	Mus musculus transcribed sequences	2.27	0.00125
BG071839		Mus musculus transcribed sequences	2.254	0.00124
BG071694	AK087752	Mus musculus transcribed sequence	2.163	0.00857
BG071895	CJ089285	Mus musculus transcribed sequence	2.158	0.000687
BG075929	AB093236	RIKEN cDNA 4932439K10 gene	2.122	0.000735
BG071108	AK050767	expressed sequence AA407809	2.058	0.000379
BG074130	BC059809	RIKEN cDNA 2410016O06 gene	2.02	0.00104
BG077636	AK154249	RIKEN cDNA 1500003D12 gene	2	0.00557
BG066520	BC016266	RIKEN cDNA 1500005G05 gene	1.994	0.00695
BG084373	XM_358382	RIKEN cDNA E130119P06 gene	1.959	0.00531
BG071520	AU043288	Mus musculus transcribed sequences	1.949	0.00129
BG066094	AK147653	Mus musculus transcribed sequences	1.884	0.00752
BG078087	BC061110	RIKEN cDNA 2810055C14 gene	1.859	0.000702
AU045922	AK008402	DNA segment, human DXS9928E	1.845	0.00337
BG066096		Mus musculus transcribed sequences	1.803	0.00068
BG071286	CB946057	RIKEN cDNA 1810037I17 gene	1.761	0.00712
BG065399	AK039840	RIKEN cDNA 2900010J23 gene	1.73	6.43E-05
BG066118	BC011270	RIKEN cDNA 2810457M08 gene	1.705	0.00748
BG084367	AK122299	RIKEN cDNA 6430548M08 gene	1.682	0.00734
BG063439	CA481515	RIKEN cDNA 0610009D10 gene	1.678	0.00734
BG066164		Mus musculus transcribed sequences	1.652	0.00961
BG066180		Mus musculus transcribed sequence	1.626	0.00269
BG066198	AK162053	RIKEN cDNA 2410016F19 gene	1.6	0.00441
BG079551	AK019681	RIKEN cDNA 4930517K11 gene	1.573	0.00285
BG063347	AK077600	RIKEN cDNA 5730466P16 gene	1.554	0.00087
BG066039	AK051745	Mus musculus transcribed sequence	1.507	0.00445
BG069651	BC060624	RIKEN cDNA 2610510H01 gene	0.736	0.00973
BG063746		RIKEN cDNA 4933407E01 gene	0.694	0.00288
BI076418	BC022950	RIKEN cDNA 1600029D21 gene	0.689	0.00491
BG073874	NM_029432	RIKEN cDNA 4930402H24 gene	0.663	0.00839
BG088717	BC033365	RIKEN cDNA 6330407G04 gene	0.658	0.00209
AU040419	AK142753	RIKEN cDNA 4933439F18 gene	0.656	0.00393
BG070393	AK085228	Mus musculus transcribed sequence	0.654	0.0079
BG070573	BC043118	cDNA sequence BC043118	0.651	0.0095
BG063463	AK141844	RIKEN cDNA 4432409D24 gene	0.651	0.00311
BG073906	AK128996	RIKEN cDNA 9030414M07 gene	0.628	0.000527
BG073203	BC094385	RIKEN cDNA 5033428A16 gene	0.619	0.00757
AU040379	BC043095	AU040379 Mouse four-cell-embryo cDNA	0.619	0.00524
BG070000	BC103802	RIKEN cDNA 2700016E08 gene	0.617	0.0082
BG074549	BC056466	RIKEN cDNA 9530019H02 gene	0.608	0.00279
BG073048	AK004717	RIKEN cDNA 1200011O22 gene	0.606	0.00997
BG069537	BC062190	cDNA sequence BC026590	0.596	0.00692
BG067288	AK159032	RIKEN cDNA 4930544L10 gene	0.594	0.00126

Clone ID	Genbank ID	Common	Fold Difference	P value
BG067613	AK141844	RIKEN cDNA 4432409D24 gene	0.584	0.0011
BG088066	AK164818	expressed sequence AW547365	0.58	0.00192
BG087082	AK050177	hypothetical protein MGC6357	0.562	0.000815
AU042062	XM_134537	RIKEN cDNA 2310061F22 gene	0.561	0.00477
BG072294	XM_619997	Mus musculus transcribed sequence	0.557	0.00792
BG076494	AK037538	RIKEN cDNA 1110032N12 gene	0.556	0.00466
BG064084	AK034483	RIKEN cDNA 2310016N05 gene	0.554	0.00205
BG067516	AK146771	RIKEN cDNA 2410004P19 gene	0.548	0.00565
AW539636	AK034817	Mus musculus transcribed sequence	0.546	0.00629
BG080662	AK154818	RIKEN cDNA D930015E06 gene	0.537	0.00181
BG081572	AK089209	RIKEN cDNA 4931433E08 gene	0.536	0.0071
BG075873	BC086617	RIKEN cDNA 2810442O16 gene	0.535	0.00111
BG075924	AK030957	DNA segment, Chr 15, Wayne State Uni 75	0.533	0.00915
BG071149	AK044190	Mus musculus transcribed sequence	0.525	0.00667
BG077491	AK140643	RIKEN cDNA 4933427L07 gene	0.525	0.000678
BG085405	AK046883	cDNA sequence BC017607	0.503	0.00929
BG069846	BC054080	expressed sequence AI043120	0.503	0.0036
BG080013	AB093261	RIKEN cDNA 4930506D01 gene	0.501	0.00425
BG071250	XM_204439	expressed sequence AI316885	0.499	0.00168
AW547680	NM_001025608	Mus musculus transcribed sequence	0.48	0.00304
BG069332	AK147085	RIKEN cDNA 4432405K22 gene	0.473	0.00203
BG076080	XM_358330	cDNA sequence BC013720	0.468	0.00246
BG068645	BQ177910	Mus musculus transcribed sequences	0.442	0.00246
BG076130	BC063749	Mus musculus 0 day neonate head cDNA	0.431	0.00731
BG086326	AK035840	RIKEN cDNA 9030624J02 gene	0.427	0.000542
BG085556	AK137588	RIKEN cDNA 8030445B08 gene	0.42	0.00239
BG082308	BC055046	RIKEN cDNA 9530020G05 gene	0.409	0.00606
BG074005	NM_172843	RIKEN cDNA 1110020D10 gene	0.409	0.00272
BG085756	AK036931	RIKEN full-length enriched library, clone:A530085C22	0.374	0.00186
BG069142	AK047485	Mus musculus transcribed sequences	0.37	0.00437
BG077451	AK043420	RIKEN cDNA 1110021N07 gene	0.367	0.00183
AW537151		G0112H12-3 NIA Mouse E7.5 Embryonic Portion cDNA L	0.362	0.00881
BG083353	XM_485962	RIKEN cDNA 4632434I11 gene	0.362	0.00131
C85340	AK170710	RIKEN cDNA 1110059P08 gene	0.345	0.00188
BG075363	AK170682	RIKEN cDNA 9630015D15 gene	0.325	0.0058
BG088526	AK028983	RIKEN cDNA 9030425E11 gene	0.322	0.00171
BG070499		RIKEN full-length enriched library, clone:A530085C22	0.304	0.00472
BG086786	NM_172277	RIKEN cDNA B130023O14 gene	0.252	0.00173

Table 2S- ESTs identified in highly metastatic epithelial cells. Microarray profiling of transcript alterations in immunopurified epithelial cells from primary tumors that metastasize to lung and bone when compared to weakly or non-metastatic tumors. Fold difference indicates expression in highly metastatic tumors over expression in weakly or non-metastatic tumors (>1 represents over-expression and <1 indicates genes that are suppressed in highly metastatic tumor cells).